UNIVERSITY OF OKLAHOMA
GRADUATE COLLEGE

ENERGY PERFORMANCE STUDY OF HEATING, COOLING, AND HOT WATER SYSTEM INTEGRATED WITH THE LATENT HEAT THERMAL ENERGY STORAGE IN DIFFERENT U.S. CLIMATE ZONES

A THESIS
SUBMITTED TO THE GRADUATE FACULTY
in partial fulfillment of the requirements for the
Degree of
MASTER OF SCIENCE

By
EMMNAUEL HAKIZIMANA
Norman, Oklahoma
2020

ENERGY PERFORMANCE STUDY OF

HEATING, COOLING, AND HOT WATER

SYSTEM INTEGRATED WITH THE LATENT HEAT THERMAL ENERGY

STORAGE IN DIFFERENT U.S. CLIMATE ZONES

A THESIS APPROVED FOR THE
SCHOOL OF AEROSPACE AND MECHANICAL ENGINEERING

BY THE COMMITTEE CONSISTING OF

Dr. Li Song, Chair

Dr. Hamidreza Shabgard, co-Chair

Dr. Jie Cai, 3rd committee member

Acknowledgment

Foremost, praised be the LORD God Almighty for His love, mercy, care, and protection to my committee members and me through the COVID-19 pandemic and all the time. A great and wonderful God continues to sustain me every day. Glory to Him (God), who lives forever.

I would like to express my sincere gratitude to my master's thesis advisors, Dr. Li Song, and Dr. Hamidreza Shabgard. Prof. Song accepted me into her lab and trained and encouraged me to be a better technical writer, a researcher, and a better academic version of me. Her guidance, endless patience, and infinite support have intellectually shaped me, supported my growth, and inspired me to complete this work. My sincere gratitude to Dr. Hamidreza Shabgard, co-advisor, for his patience and guidance. Without both Prof. Song and Dr. Shabgard, this thesis work would not have come to completion. Special thanks to Dr. Jie Cai for accepting to be on my committee member. I look up to him for his gentleness and caring. I am deeply motivated to take up his example.

I would like to express my special thanks to Prof. Mistree for his friendship. Words cannot express how grateful I am. His impact and selfless support would be my legacy forever.

For two years, many people have been helpful to color my life both academically and socially. I would like to thank my colleague at the graduate student community. They have believed in me and nominated me to be the co-chair for one and a half years. Not only have I gained leadership experience, but also I

got an opportunity to develop networking. Further, I would like to acknowledge fellow students from building energy efficiency laboratory. Their support was essential to me.

Lastly, I express my sincere appreciation to my family for their love and support throughout, especially my brother Alphonse Mugenzi. Special thanks to my girlfriend and my best friend Jennymae Joseph, who encourages me always to give my best. Special thanks to my church family at Norman seventh day Adventist. Glory be to God who brought you into my life.

Table of Contents

Table of Contents

List of Tables

List of Figures

List of Figures

Definition of the Terms

Q	energy (kWh)
$load$	heating, cooling, and hot water loads (kWh)
$A_{collector}$	collector surface area (m^2)
COP	coefficient of performance
GHI	global horizontal index
HP	heat pipe
HVAC	heating, cooling, and air conditioning
LHTES	latent heat thermal energy storage
HX	heat exchanger
ODE	ordinary differential equation
PCM	phase change material
TMY	typical meteorological year
TES	thermal energy storage (kWh)
ASHRAE	American Society of Heating, Refrigerating and Air-Conditioning Engineers
SEER	the seasonal energy efficiency ratio
EER	energy efficiency ratio
h	hour
d	day
T	temperature (K)
T_{PCM}	PCM temperature (K)
h_{sl}	the heat of fusion (kJ/kg)
m	mass (kg)
m_{PCM}	PCM mass (kg)
α	LHTES energy saving ratio
β_{solar}	solar utilization ratio
spm	saving per PCM mass
spa	saving per area
$\eta_{collector}$	collector efficiency
c	specific heat (J/kg K)
cp	Specific heat capacity (J/kg K)
E	thermal element
Ex	exergy(kJ)

H	height of PCM compartment (m)
k	thermal conductivity (W/m K)
k_{PCM}	thermal conductivity of the PCM (W/m K)
k_s	thermal conductivity of metal in the metal foam (W/m K)
L	input (output) hp spacing (m)
M	related to the number of the PCM thermal elements in the solid region
N	number of PCM thermal elements in the liquid region
q	heat transfer rate (W)
r	radius (m)
S	entropy (kJ/kg K)
s	melting front location (m)
T_b	the temperature at the interface of PCM regions around input and output heat pipes (K)
$T_{i,n}$	the temperature at the interface of PCM thermal element E_n and E_{n+1}(K)
T_m	PCM melting temperature(K)
T_n	the temperature of the elements E_n calculated in the middle of the element (K)
T_w	metal wall temperature (K)
V_f	melt volume fraction
V_l	melted PCM volume (m^3)
δ	thermal element half-thickness (m)
ρ	density (kg/m^3)
ϵ	Porosity
ϕ	generic variable

ABSTRACT

An energy performance study of a new solar thermal-powered heating, cooling, and hot water system, integrated with a latent heat thermal energy storage (LHTES) and applied in cities in different climate zones (or regions) across the United States, is conducted. A mathematical model was developed and simulated using MATLAB to determine the energy demands with and without the LHTES. Seven cities were selected in seven different U.S. climate zones. For each city, the daily building energy demand, daily global horizontal index (GHI), solar collector area, and thermal energy storage size were calculated. To evaluate the capabilities and benefits of the LHTES system, the annual building energy demand with and without solar collector and thermal energy storage, energy cost savings, annual energy savings per unit PCM mass of thermal energy storage, energy savings per unit area of the collector and solar energy utilization ratio was calculated. Results show that the LHTES system is capable of reducing energy demands for residential buildings in all the seven climate zones; however, the system is more beneficial in warmer climate zones than in colder climate zones. In warmer climate zones, the equipment sizes are smaller, the annual energy savings per unit mass of thermal energy storage is larger, energy savings per unit area, energy cost savings, and solar energy utilization ratio are higher than in colder climate zones indicating that LHTES system are more beneficial in warmer climate zones than in colder climate zones. Nevertheless, further research should be conducted to carefully investigate the capital cost and affordability of the system to initiate the deployment of the LHTES system in the HVAC industry.

1. THE BACKGROUND OF THE PROJECT

In this thesis, the energy performance study of a novel solar thermal-powered heating, cooling, and hot water system, integrated with latent heat thermal energy storage (LHTES) system is conducted. The LHTES system serves thermal energy storage and supply heating, cooling, and hot water loads in residential buildings. An electric or natural gas heater can be used as a backup for times when solar energy is not sufficient or not available, providing a versatile heating source with minimum extra cost [1]. In this chapter, the layout of the heating, cooling, and hot water system integrated with latent heat thermal energy storage is presented first; then, the components of latent heat thermal energy storage are discussed; and lastly, the research objectives and thesis overview/organization are summarized.

1.1. The System Layout

The layout of the solar-thermal powered heating, cooling, and hot water system integrated with the latent heat thermal energy storage is shown in Figure 1.1. The system includes an evacuated glass tube solar collector, a home absorption air conditioning unit or heat pump unit, and a latent heat thermal energy storage (LHTES) unit. The LHTES unit is composed of three heat exchangers and a PCM (phase change material) compartment connected to a glass tube collector by heat pipes. The three heat exchangers serve to generate saturated vapor for absorption

air conditioning, produce hot air for space heating (not needed if an absorption heat pump is employed), and supply hot water for domestic applications.

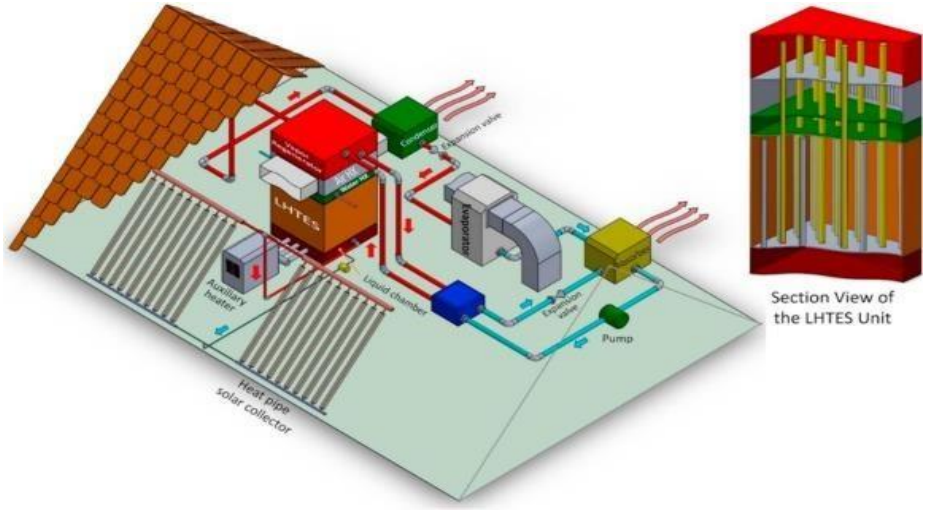

Figure 1.1. The view of the combined solar heating, cooling, and hot water with latent thermal energy storage (adopted from [1]).

The solar radiation is absorbed on the outer surface of the solar collector and vaporizes the liquid working fluid inside the pipes. The created saturated vapor leaves the collector pipes from the top. It is then passively driven to the LHTES unit due to induced pressure difference between the relatively hot (collectors) and relatively cold (LHTES unit) sides. Inside the LHTES unit, the vapor rises the input heat pipes, where it condenses due to heat transfer to the relatively colder PCM regions. The evacuated tube collectors, the condensation pipes inside the PCM, and connecting tubes create a heat pipe loop in which the collectors serve as the "evaporator" section, and the tubes penetrating the PCM act as the "condenser" section [1].

1.2. The Components of the LTHES System

The proposed LTHES system is made up of evacuated tube solar collectors, latent heat thermal energy storage unit with three heat exchangers for an absorption air conditioning unit or heat pump (not shown in this thesis), a solar-assisted water heater unit, and a space heating unit (not needed if the heat pump is used). The comprehension of an individual unit in the system can serve as a guide to selecting equipment for experimentation or motivate the interested researcher to seek more information. As such, the brief functionality of each unit is presented in this section.

1.2.1. The evacuated tube solar collector

The evacuated tube solar collectors (ETCs) convert solar energy into thermal energy for domestic and commercial hot water heating, pool heating, space heating, air conditioning, etc. ETCs consist of evacuated tubes with two evacuated hollow glass tubes connected to heat transfer fin through which thermal energy is transferred by heat pipes to the manifold [2].

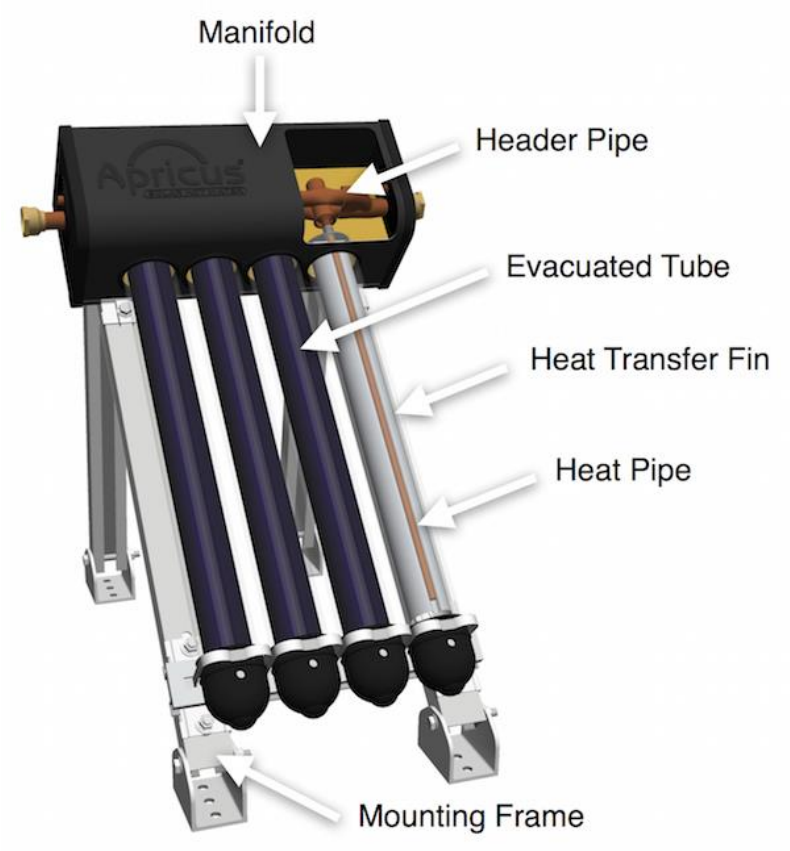

Figure 1.2. A schematic of an evacuated tube solar collector (adopted from [2]).

Evacuated hollow glass tubes create excellent insulation, trapping the heat inside the tube, making evacuated glass tubes highly efficient [3]. The solar selective coating absorbs solar energy and conveys it to the heat pipes which are located inside the inner tubes. The heat pipe contains a heat transfer fluid (typically water or ethylene glycol), which is the medium to transfer thermal energy to the manifold. The boiling temperature of the liquid inside the heat pipes is coupled with the internal pressure of the heat pipes. Applying heat to the heat pipes leads to the vaporization of the liquid working fluid inside the heat pipes. The vapor then rapidly rises to the top of the heat pipe while carrying a large amount of energy to the manifold. As the heat is off-loaded to the manifold (and then to the LHTES

unit), the vapor condenses, and liquid returns to the bottom of the heat pipe, creating a loop. An aluminum fin, held in the tube by a spring clip, facilitates heat transfer, and mechanically supports the heat pipe in place [4].

1.2.2. The latent heat thermal energy storage unit

The latent heat thermal energy storage unit is shown in Figure 1.3. Thermal energy storage is connected to the solar collector by heat pipes running from ETCs manifold to the bottom section of the LHTES unit. The unit is comprised of input heat pipes, output heat pipes, PCM chamber (space separating input and output heat pipes filled with choice PCM), and heat exchanger chamber (right above the PCM chamber).

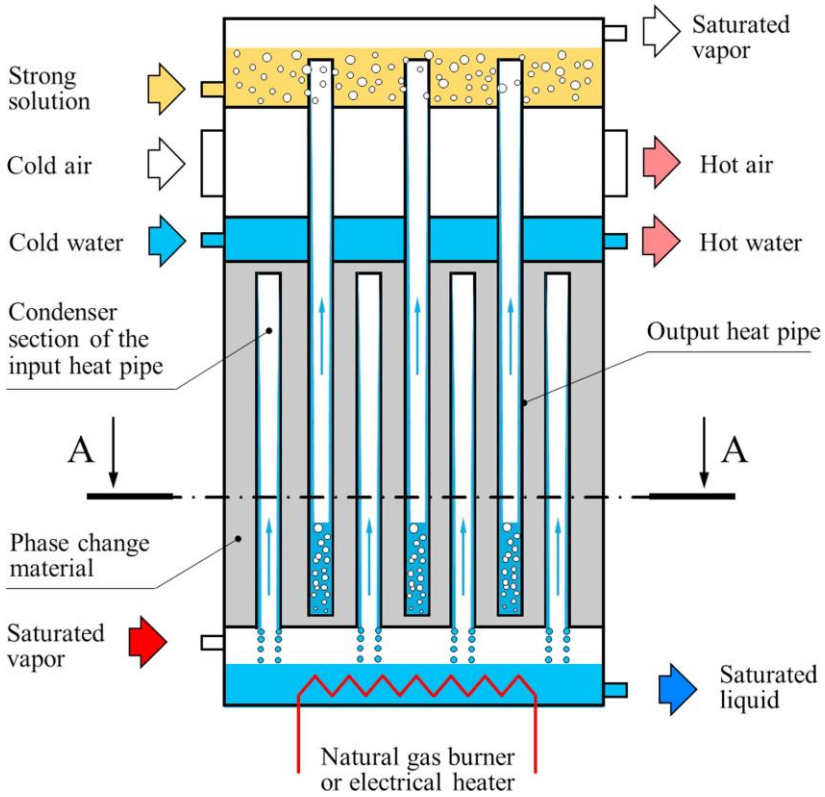

Figure 1.3. Schematic of the LHTES system showing the condenser section of the input heat pipe, output heat pipes, and related heat exchangers (adopted from [1]).

The PCM is a substance with a high heat of fusion which, when melted and solidified at a specific temperature, can store and release a large amount of energy [5]. The Input and output heat pipes are made of stainless steel [1]. The PCM is impregnated in aluminum metal foam to improve melting and solidification rates [6]. Thermal energy flow starts the solar collector, by which from thermal energy absorbed vaporizes liquid working fluid into a saturated vapor (shown by the left-bottom red arrow) to the bottom of the LHTES unit. The saturated vapor then accumulates into the condenser section of the input heat pipes. Saturated vapor creates a temperature difference between the condenser section of input heat pipes and the neighboring PCM thus heat is transferred through PCM to output heat

pipes. The thermal energy transferred through the PCM is eventually transported to the three heat exchangers via output heat pipes. A natural gas burner is used as an auxiliary energy supply when solar energy is not sufficient or not available.

1.2.3. Space heating

Space heating can be achieved in two ways, i.e., by using the heat pump unit or by allowing air through the middle sections of heat exchangers of the LHTES unit (see Figure 1.3). The former (heat pump) method eliminates the air heat exchanger, thus helps reduce the volume of the LHTES unit. To achieve space heating with the former method, the air handling unit can be used to re-condition and circulate air to the building [7]. The hot air produced can be distributed to different spaces/rooms in the house.

1.2.4. Solar assisted water heater unit

Hot water is prepared by passing domestic city (cold) water through the hot water heat exchanger inside the LHTES unit shown in Figure 1.2. Domestic city water passes through the thermal energy storage unit where water flows normal to the surface of output heat pipes in the water heater heat exchanger, thus absorbs heat. Hot water then flows down into the storage tank and can be used when needed. The water flow rate can be regulated to maintain the outlet temperature within the desired range above the minimum temperature [8].

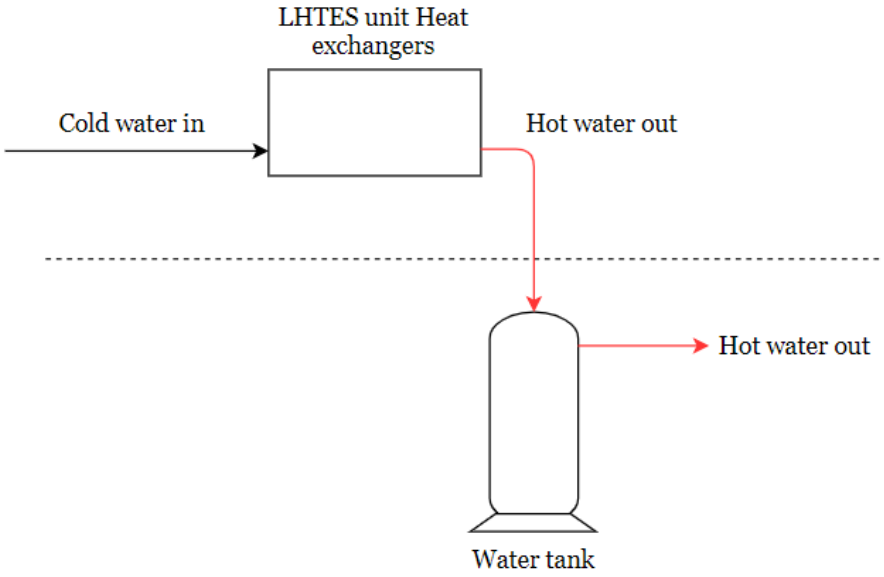

Figure 1.4. Hot water preparation loop in latent heat thermal energy storage system

1.3. Research Objectives

In the course of the thesis, the main objectives will help in setting the milestones and planning for the project. The objectives of this research are:

1. To simulate the heat transfer and building energy for solar thermal powered heating, cooling, and hot water system integrated with latent heat thermal energy storage on an annual basis (i.e., 365 days).
2. To evaluate the feasibility and the benefits of the solar thermal powered heating, cooling, and hot water system integrated with the latent heat thermal energy storage (LHTES) by analyzing and evaluating energy performance in residential buildings for different climate conditions.

1.4. Thesis Overview/Organization

This thesis aims to obtain the different research objectives by formulating a mathematical model of a solar-powered LHTES system. The research objectives boil down to determining the capabilities of the LTHES by calculating energy captured by a solar collector, total building energy demand, and how much auxiliary heating required when solar energy is not enough or not available. The following chapters are organized as below:

Chapter 1. The background of the project. In this chapter, a knowledge of the Heating, Ventilating, and Air-conditioning (HVAC) and hot water System integrated with LHTES system is presented. In the end, the research objectives and thesis overview/organization are presented.

Chapter 2. The literature reviews. In this chapter, the findings from the literature search and review are presented. It is purposed to show the state of the art of the LHTES system and provide research gaps addressed in this thesis.

Chapter 3. LHTES system mathematical modeling and equipment sizing. In this chapter, the employed time-dependent one-dimensional heat transfer model is presented. Besides, the climate zones (in which candidate cities are selected) are explained, and equipment sizes required in each candidate cities are presented.

Chapter 4. LHTES system heat transfer and energy performance analysis. In this chapter, the heat transfer, exergy, and building energy simulation results are presented. Also, the annual building energy cost and the LHTES system energy

performance evaluation are analyzed to propose the benefit of the LHTES system in different climate zones.

Chapter 5. Closing remarks. This is the last chapter of this thesis. In this chapter, conclusions and future work are provided.

2. LITERATURE REVIEWS

Buildings account for approximately 40% of the worldwide annual energy consumption. Fossil fuels (non-renewable energy) satisfy most of the energy demands; thus, they contribute significantly to global warming. The measures to alleviate fossil fuels' impact on global warming should include offsetting the building energy demand using renewable energies [9]. Among the renewable energies available, solar energy is deemed the best option because of its affordability, accessibility, and prevalence [10].

In the United States, the net renewable energy production accounts for about 17.7%, out of which 2.0% is solar energy (see Figure 2.1). The rest of these renewable energies come from hydropower, wind, geothermal, and biomass. Thus, there is a need to harness the solar energy [11].

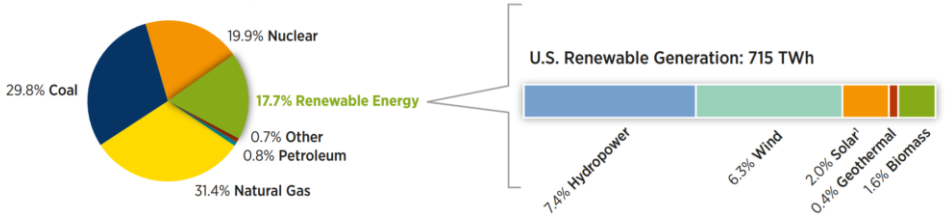

Figure 2.1. The U.S electricity nameplate capacity and generation. (The distributions of various categories of energy under renewable generations in the U.S) (adopted from [11]*).*

In this chapter, the literature review intends to explore ways to harness solar energy in an economical way possible and present the gaps (novelty) addressed by this study.

2.1. State of Art

The proposed LTHES system is an integration of several mature technologies: solar collector, thermal energy storage, and absorption A/C. The extensive literature review has revealed the existence of combination of the latent heat thermal energy storage with only space heating, space cooling, hot water system, heat pump, absorption air condition unit, or the combination of two different units and no study has put all the three or more together. Further, a current survey of an integrated system simulates the heat transfer and exergy of the system for a cold day and a hot day. Therefore, there is a need to include building heating, cooling, and hot water loads using the heat transfer and exergy model and carry out a simulation for the entire year (i.e., 365 days). As a result, blending in the building load and simulating the LHTES performance for the whole of the year sets in the innovative approach and is the focal point of this study. Each component of the system categorizes the literature review.

2.1.1. Glass tube solar collector

According to SEIA, solar energy is the cleanest and the most abundant renewable energy source available; the U.S. has some of the most abundant solar resources in the world. Solar technologies can harness this energy for a variety of uses, including generating electricity, providing light or a comfortable interior environment, and heating water for domestic, commercial, or industrial use. There are two different ways to harness solar energy, namely photovoltaics and solar

thermal systems. Solar thermal systems are categorized into relatively low-temperature non-concentrating systems (e.g., solar chimney, flat plate, and evacuated tube collectors), and concentrating solar power [12].

Photovoltaic (PV) is a system that uses solar cells to convert solar energy into electricity. The PV cells used by the Photovoltaic (PV) system entail two layers of materials that are semi-conductors in nature made from silicon. When the cells receive direct sunlight from the sun, they create an electric field on the segments, which will generate a flow of electricity. When the intensity of the light from the sun increases, then the flow of electricity on the surface increases [13].

The Photovoltaic (PV) systems require the need for special energy converters or maximum power point tracking (MPPT) converters that can provide maximum energy yield [14]. Environmental and operational stresses, such as humidity, temperature, and high-voltage bias, and process limitations, such as solder bond integrity, affect PV modules, and the balance of the system (BOS) components, including power conditioning systems, in the same fashion giving rise to corrosion, electro corrosion, solder bond coarsening, etc. [15]. PV systems are not favored because of their high cost, low efficiency, and fast deterioration [16].

An alternative way of harnessing solar energy is by using concentrating solar power (CSP). Concentrated solar power is a system that is used to generate solar power by utilizing lenses and mirrors to concentrate a stream of light into one area in the form of a receiver. Consequently, this leads to the generation of electricity as a result of the conversion of solar energy into thermal energy.

Nevertheless, CSPs are not favored because they are limited to arid climates[17], utilize only a direct normal portion of solar radiation (i.e., diffuse radiation cannot be concentrated), operates at a low thermal cycle efficiency [18], and expensive [19].

Besides PV and CSP, other options to harness solar energy are non-concentrating solar thermal systems such as solar chimneys, flat plates, and evacuated glass tube collectors. (1) A solar chimney is a solar power generating facility, which uses solar radiation to increase the internal energy of air flowing through the system, thereby converting solar energy into kinetic energy. The kinetic energy from the wind is then transformed into electricity by the use of a suitable turbine [20]. One of the main disadvantages of solar chimneys is their (2) flat plates have the solar absorbing surface approximately equal to the overall collector area that intercepts the sun's rays. Both solar chimney and flat plate solar collectors possess very low efficiencies [21]-[22]. (3) Evacuated tube collectors (ETCs) are favored because they possess vacated space, which reduces convection and conduction losses, thus enhance thermal performance [23]. In addition, ETCs systems have high efficiency at a low angle of incidence [24] and are economical [25].

2.1.2. Latent thermal energy storage and the phase change material (PCM)

Thermal energy storage is classified as sensible heat storage (SHS), latent heat thermal energy storage (LHTES), and thermochemical energy storage (TCES). In TCES, thermal energy is used to drive a reversible endothermic

chemical reaction, storing the energy as chemical potential. During periods of high solar insolation, an energy-consuming reaction stores the thermal energy in chemical bonds; when energy is needed, the reverse reaction recombines the chemical reactants and releases energy. Latent heat thermal energy storage involves phase transformation of the storage material from one state to another, such as solid-liquid, solid-solid, or liquid-gas and vise-versa when heated to the transformation temperature. A liquid-gas transition requires a large volume of material conduit, while a solid-solid transition involves low energy storage density per unit volume of material. Therefore, the solid-liquid transition as applied to latent heat storage applications is more efficient compared with the other transformations and hence, is the most widely used. On the other hand, SHS resembles latent heat thermal energy storage; however, it does not involve phase transformation [26] - [27].

Nasiru et al. report that sensible heat storage requires a larger vessel as compared with latent heat and thermo-chemical storages [28]. Thermochemical storage, on the other hand, is associated with high energy storage density but still at the pre-matured stage in terms of research and development. Among the three thermal energy storage methods, latent heat energy storage is the most promising and attractive due to its compactness and ability to store energy at the nearly constant temperature corresponding to the phase-transition temperature of the material. PCM thermal storage improves energy efficiencies by limiting the

discrepancy between the energy supply and the energy demand for solar thermal energy applications [29].

Several other kinds of research were conducted on the practical storage of solar energy using phase change materials (PCM). Beatrice Castellani et al. studied the application of clathrate hydrates as PCM in buildings. Clathrate hydrates are crystalline structures in which guest molecules are enclosed in the crystal lattice of water molecules. Castellani observed that clathrate hydrates have potential in terms of improving indoor thermal comfort and reducing energy consumption for cooling [30]. Kaygusuz et. al investigated the thermal characteristics of paraffin or expanded perlite (paraffin/EP) composite for latent heat thermal energy storage. The form-stable paraffin/EP composite PCM was prepared as a novel energy storage material for LHTES applications. The paraffin as PCM was confined in the porous EP by the mass fraction of 55% without melted PCM seepage, and the mixture was described as form-stable composite. The melting and freezing temperatures and latent heats of form-stable composite PCM were determined as 42.27°C and 40.79°C and 87.40 J/g and 90.25 J/g, respectively [31].

A handful of techniques for heat transfer enhancement were investigated to improve the thermal performance of the LHTES system. The enhancement techniques include the enhancement with fins to increase the heat transfer area between PCM and heat exchangers [32]; the application of metallic inserts in heat storage PCM-based units to improve thermal conductivity [33]; extended surfaces and encapsulation of PCM to increase heat transfer surface area [34];

Impregnation of porous metal foam to enhance the thermal conductivity of conventional PCMs in LHTES systems [35]; dispersion of nanoparticles/high conductivity materials such as aluminum powder and carbon nanoparticles to paraffin wax to improve thermal conductivity [36]-[37]; distribution of low-density materials such as carbon fibers to improve the transient thermal response and thermal conductivity [38]; and combining two different enhancement techniques viz. using multiple PCMs and addition of fins to increase the rate of melting PCM [39] and integration of heat pipes with and without metal foams and foils to improve heat transfer rate [40] - [41].

In this research, magnesium nitrate hexahydrate (used as PCM) is embedded in an aluminum metal foam. Even though the inclusion of metal foam suppresses the natural convection significantly, the improved effective thermal conductivity more than offsets the effect of weakened natural convection. As such, the addition of metal foams substantially enhances the heat transfer rate within the PCM [1].

2.1.3. Absorption Refrigeration Cycle

Several types of research have been conducted on the solar thermal-driven absorption refrigeration cycle. Mittal et al. [42] conducted a performance analysis of several working fluids. They found out that among the major working fluids available, LiBr/H2O is better suited for solar absorption air-conditioning applications over ammonia/water because of the higher coefficient of

performance. Omar Ketfi et al. investigated the performance of a single effect solar absorption cooling system utilizing LiBr/H2O as the working fluids. In his research, he observed that the COP of the cycle increases with increasing the generator and the evaporator temperatures. At the same time, it decreases with the increase in the condenser and the absorber temperatures [43].

Alternatively, Oliver Marc et al. conducted a study on dynamic modeling and experimental validation elements of a 30 kW LiBr/H2O single-effect absorption chiller for solar application on which he concluded that the model predicts with reasonable accuracy the outlet temperatures of the generator, the cooling loop (absorber and condenser) and the evaporator, whatever the inlet temperatures are[44].

In this thesis, LiBr/H_2O is used as a liquid working fluid for absorption heating, cooling, and air conditioning or a heat pump. LiBr/H_2O has low specific heat (c_p), thus the high coefficient of performance.

2.1.4. Integrated LHTES system in residential building

The recent concentrations of greenhouse gases in the atmosphere are vastly increasing due to increasing energy consumption in all sectors, from transportation to buildings. Buildings have a dominant contribution to global energy use, accounting for about 40% of the total energy consumption. They are responsible for over 30% of the CO_2 emissions, and a large amount of this energy is exhausted to provide thermal comfort in buildings, explicitly heating, cooling,

and air conditioning system. These systems consume a large amount of energy; thus, they have harmful effects on human health and the natural environment and cause significant problems at peak energy load time. Therefore, alternative sustainable strategies such as thermal energy storage (TES) can replace or at least mitigate the increasing demand for these systems in buildings by preserving the available energy at a time of surplus to be extracted and used during the unavailability period [45]. Thermal energy storage is essential technologies for decarbonization and constitutes a convenient way to store thermal energy in the building by utilizing PCMs [46]. Residential buildings have been identified as one of the few sectors that have the potential to see considerable energy savings through the utilization of renewable energy and green building concepts [47].

Kossecka and Kosney conducted a study on the thermal balance of a wall with PCM enhanced thermal insulation. In their study, the performance of the PCM-enhanced insulation in different climate conditions was simulated on a lightweight wall assembly with PCM-enhanced insulation under different external thermal excitation. It was found that the heat gains maxima, resulting in high cooling loads, are shifted in time by about two hours and reduced up to 22% for not very high external sol-air temperatures[48].

Hawes et al. investigated impregnating the PCM into building materials such as wallboard and concrete block [49]. This combination offers a wide range of benefits, including saving energy in building, easy experimentation and application and manufacturing cost-effective. Castellon et al. conducted an

experimental study of PCM inclusion in the different building envelopes. It was observed that impregnating building envelopes with PCM could achieve an improved thermal comfort without a substantial increase in the weight of construction material. For instance, the indoor temperature fluctuation was reduced, the peak temperature was shifted, and the energy consumption of the HVAC system was reduced [50].

In another research, Nattaporn Chaiyat studied the concept of using phase change material for improving the cooling efficiency of an air conditioning unit in Thailand. Nattaporn compared the efficiency and energy performance of the air conditioner with and without PCM. The modified system, i.e., the system with PCM, was found to reduce about 9% of electricity use per day [51].

In other researches, Mehmet conducted an experimental investigation to validate a solar-aided latent heat thermal energy storage for space heating by the heat pump to determine monthly space heating loads, stored energy, and total solar insolation on solar collector surface and compare it with the simulation results [52]. The simulation and experimental results agreed in terms of PCM by volume in solid-phase transitioning to the liquid phase. Once more, Du et al. conducted experimental studies on an air-cooled two-stage solar absorption air conditioning by investigating the feasibility and performance of the prototype [53]. The study revealed a stable COP and an acceptable range of electric efficacy when the prototype is driven by hot water from 76°C to 88°C for air-conditioning.

Recently, Shabgard et al. [1] developed a heat transfer and exergy model of an integrated heating, cooling and hot water system with latent heat thermal energy storage to quantify the exergy efficiency of the system and analyze the thermal performance of a latent heat thermal energy storage system integrated with heat pipes. Magnesium nitrate hexahydrate was selected as phase change material (PCM). LHTES energy performance was analyzed for a residential building in Phoenix, AZ (characterized by hot-dry climate). One dimensional heat transfer model was developed, and the simulation was conducted for a typical cold (January 1st) and a typical hot day (July 2nd). The results showed that a latent heat thermal energy storage system with a capacity of 29kWh coupled with a 10m^2 evacuated tube collector solar collector can decrease the annual building energy by about 87%. The exergy efficiency was found to be 74% (80%) for a cold (hot) day.

2.2. Identifying the Gaps

The performance of solar HVAC and hot water systems strongly depends on solar insolation, climate conditions, and time-dependent energy demand. As such, models that predict the system performance in various climate conditions throughout the entire year are critical for the development of solar HVAC and hot water systems. There is, therefore, the need to upgrade the heat transfer and exergy model and carry out the simulation for the entire year (i.e., 365 days). Also, there is a need to blend in the calculations of auxiliary energy demand into the model and evaluate building energy performance evaluation. Until now, the integrated

system of this kind has never been applied to different US climate zones other than the hot, dry climate zone of Arizona Phoenix thus there is a need to simulate and evaluate energy performance and benefits of employing LHTES system to residential buildings in different climate zones across the United States.

In this research, the energy savings using the LHTES system is studied using the simulation of a mathematical model for heating, cooling, and hot water over the entire year. Also, the proposed method is assumed to perform differently in different climate zone because different climate zones receive a different amount of solar energy, and building energy demand differs by different building material, weather conditions, and occupant behavior [54]-[55]. As such, an assessment of the energy performance of the system in different climate zones across the United States is needed. Further, the study of evaluation of the system performance in different climate zones could provide a knowledge base for the deployment of the solar-thermal driven cooling, heating and hot water systems integrated with latent heat thermal energy storage.

3. LHTES SYSTEM MATHEMATICAL MODELING AND EQUIPMENT SIZING

A mathematical model (based on the concept of the thermal element network for parametric studies) is presented in this chapter. The following assumptions are made in the development of the model: constant thermophysical properties, conduction-controlled melting and solidification in the PCM-metal foam, negligible thermal resistance associated with pool boiling and condensation and evaporation inside the HPs, the negligible pressure drop across the HPs, negligible heat loss, well-insulated separating plates between the heat exchangers, and negligible contact thermal resistances. Thus, heat transfer is the only mechanism for exergy transfer across the boundaries in this model. A simplified system-level mathematical model is adopted from [1] and presented first. Then, the cities on which this study is conducted and the concise approach to sizing the equipment (solar collector area and thermal energy storage) required for each city are presented.

3.1. Mathematical Heat Transfer and Exergy Modeling

A cross-section view of the LHTES unit (cross-section A-A in Figure 1.3) is shown in Figure 3.1. The unit cell is decomposed into a 1D cell (shown in Figure 3.1). 1D cell is comprised of the two pipes (condenser section of the input heat pipes (HP) and the evaporator section of the output HP). Each surrounded by the annular PCM region. The outer radius of the annular PCM region in the 1D cell is

determined from the equality of the PCM mass between the 2D unit cell shown in Figure 4.1b and the converted 1D cell in shown Figure 4.1c, $r_o=L/2\pi$. It is assumed that the outer surfaces of the annular PCM regions in the 1D cell are at the same uniform temperature T_b (Figure 4.1c). The shared surface temperature T_b varies with time as the input and output heat transfer rates change.

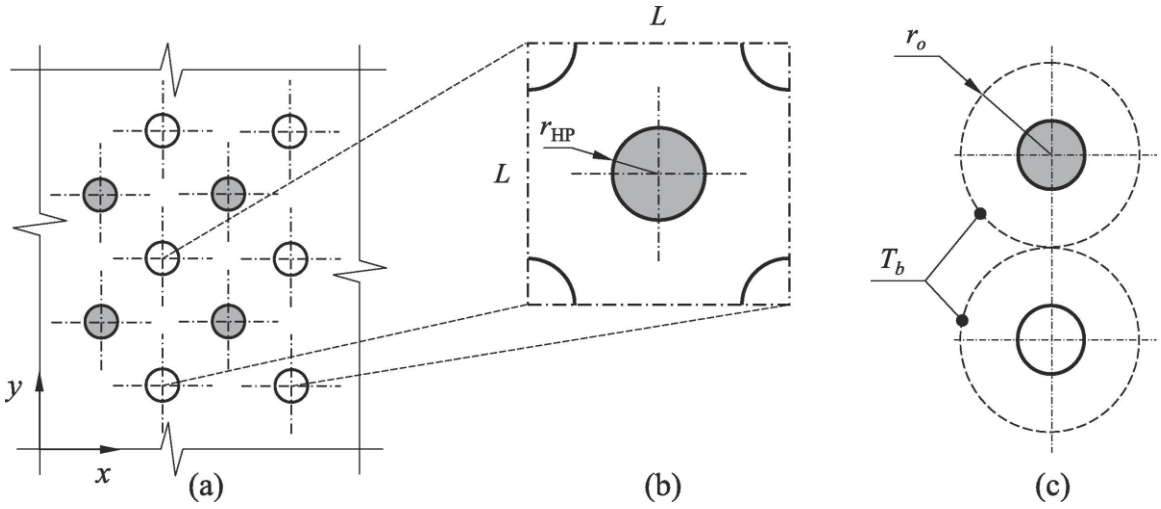

Figure 3.1. (a) A cross-sectional view of the LHTES system (along the line A-A in Figure 1.3 embedded with the condenser sections of the output heat pipe and evaporator sections of the heat pipe, (b) unit cell including one full input heat pipe and an equivalent full output heat pipe, and (c) 1D cell equivalent to the unit cell shown in the middle (adopted from [1]).

The thermal network representative of the system shown in Figure 3.1 is illustrated in Figure 3.2, and the description of each element is provided in Table 3.1. All the thermal elements in this work are annular and are characterized by a thermal resistance and a thermal capacitance. The thermal capacitance feature of the element's accounts for the time-variations in thermal energy content. In Figure 3.2a, $T_{sat,1,}$ and $T_{sat,2}$ are the saturated vapor temperatures within the input and output HPs, respectively.

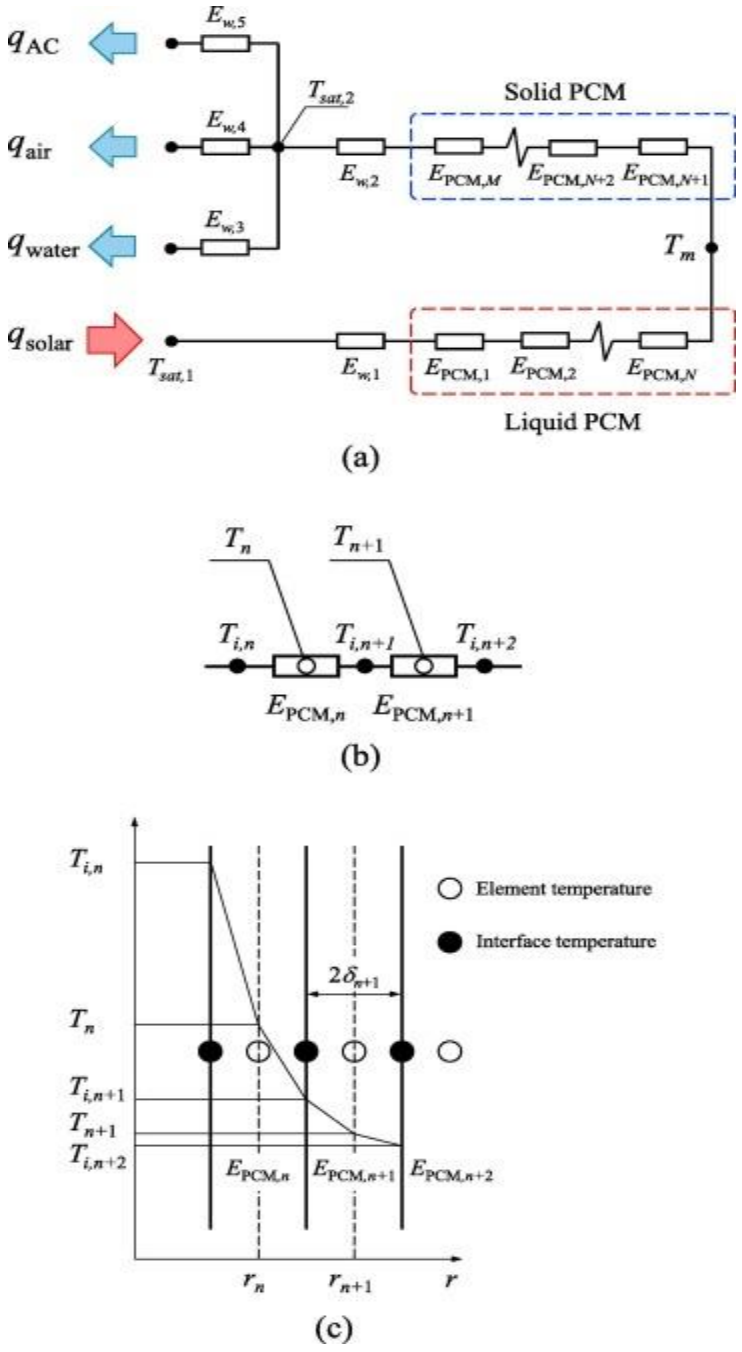

Figure 3.2. (a) Thermal resistance network for heat transfer analysis of the LHTES system and related heat exchangers, (b) definition of the element temperatures and interfacial temperatures between neighboring elements, (c) illustration of the temperature variations across elements (adopted from [1]).

Table 3.1. Description of the thermal elements appearing in Figure 4.2 (a) (adopted from [1]).

Resistance	Definition
$E_{w,1}$	Radial wall resistance and capacitance of condenser section of input HP
$E_{w,2}$	Radial wall resistance and capacitance of evaporator section of output HPs
$E_{w,3}$	Radial wall resistance and capacitance of condenser section of output HP in water HX section
$E_{w,4}$	Radial wall resistance and capacitance of condenser section of output HPs in air HX section
$E_{w,5}$	Radial wall resistance and capacitance of condenser section of output HPs in vapor-regenerator section
$E_{\mathrm{PCM},1-N}$	Resistance and capacitance of melted PCM surrounding the condenser sections of the input HP
$E_{\mathrm{PCM},\,N+1-M}$	Resistance and capacitance of solid PCM surrounding the evaporator sections of the output HPs

The energy balance for element n, E_n, is:

$$m_n c_n \frac{\partial T_n}{\partial t} = q_{n,in} - q_{n,out} \tag{3.1}$$

where m_n and c_n are the mass and specific heat of the element, respectively, and $q_{n,in}$ and $q_{n,out}$ show the input and output heat transfer rates of element E_n. The heat transfer rate into (out of) the element E_n is calculated using the difference between the element temperature T_n, calculated in the middle of the element, and the interfacial temperature between elements E_n and E_{n-1} (E_{n+1}), $T_{i,n}$ ($T_{i,n+1}$). The heat transfer surface area of the element E_n is equal to the area of the cylindrical surface passing through the middle of the element ($A_n = 2\pi\, r_n\, H$). Thus, the input and output heat transfer rates are calculated as:

$$q_{n,in} = k_n A_n \left(T_{i,n} - T_n\right)/\delta_n \tag{3.2}$$

and

$$q_{n,out} = k_n A_n \left(T_n - T_{i,n+1}\right)/\delta_n \tag{3.3}$$

The temperature of the element E_n is coupled to its neighbors through the interfacial temperatures $T_{i,n}$, and $T_{i,n+1}$. The interfacial temperature $T_{i,n+1}$, is obtained from the equality of the heat transfer rate leaving E_n and that entering E_{n+1}.

$$T_{i,n+1} = \frac{\frac{k_n A_n T_n}{\delta_n} + \frac{k_{n+1} A_{n+1} T_{n+1}}{\delta_{n+1}}}{\frac{k_n A_n}{\delta_n} + \frac{k_{n+1} A_{n+1}}{\delta_{n+1}}} \tag{3.4}$$

In this equation, k, A, and δ represent the thermal conductivity, surface area, and half-thickness of the thermal elements, respectively. It is noted that due to the difference between A_n and A_{n+1}, the temperature slope at the interface between E_n and E_{n+1} is different inside the neighboring elements despite the equality of the interfacial heat transfer rates (see Figure 3.2c).

The number of PCM elements in each of the solid and liquid regions is fixed, thus their thickness, 2δ, changes as the solid-liquid interface moves. However, when the thickness of the elements in either solid or liquid region decreases below (increases above) a critical value ($L/200$ in this work), the number of elements is reduced by half (doubled) to maintain the accuracy of the numerical results. If only one cell remains in the solid (liquid) region and its thickness decreases below the

critical value, the solid (liquid) phase completely vanishes and the liquid (solid) phase enters the superheating (subcooling) state, characterized by rapid temperature rise (drop) due to the lack of phase change. The displacement rate of the solid-liquid interface is determined from the following energy balance equation applied to the interface:

$$\rho h_{sl} \frac{dV_l}{dt} = k_N A_N \frac{T_N - T_m}{\delta_N} - k_{N+1} A_{N+1} \frac{T_m - T_{N+1}}{\delta_{N+1}} \tag{3.5}$$

where V_l is the melted PCM volume, and ρ and h_{sl} are the density and heat of fusion of the PCM, respectively. Also in Equation (3.5), T_N and T_{N+1} represent the thermal element temperatures adjacent to the phase front in the liquid and solid regions, respectively. In the above equations, the thermal conductivity of the PCM-metal foam composite [56].

$$k = \frac{\left[k_{PCM} + \pi\left(\sqrt{\frac{1-\epsilon}{3\pi}} - \frac{1-\epsilon}{3\pi}\right)(k_s - k_{PCM})\right]\left[k_{PCM} + \frac{1-\epsilon}{3\pi}(k_s - k_{PCM})\right]}{K_{PCM} + \left[\frac{4}{3}\sqrt{\frac{1-\epsilon}{3\pi}}(1-\epsilon) + \pi\sqrt{\frac{1-\epsilon}{3\pi}} - (1-\epsilon)\right](k_s - k_{PCM})} \tag{3.6}$$

where k_{PCM} and k_s are the PCM and solid matrix thermal conductivities, respectively, and ϵ is the porosity of the metal foam. An effective thermal conductivity 25% smaller than that obtained from Equation (3.6) is used in this study to account for the effects of contact resistances between the PCM and metal foam. Effective density, specific heat, and heat of fusion of the PCM-metal foam composite are calculated based on the metal foam porosity using the following generic equation:

$$\phi_{eff} = \epsilon\phi_{PCM} + (1-\epsilon)\phi_s \tag{3.7}$$

It is assumed that there is no mass transfer involved in transferring heat across Phase change material to output heat pipes. Therefore, the second energy law is stated as [57]:

$$Ex_{in} - Ex_{out} - Ex_{des} = \Delta Ex_{sys} \tag{3.8}$$

The above equation can be broken down and a detailed explanation accompanied by figures is presented. Solar is considered as the primary source of energy to avail Ex_{in} to PCM. Ex_{in} is mathematically expressed as in Equation (3.9).

$$Ex_{in} = \int_{t_0}^{t} \left(q_{solar} - T_0 \dot{S}_{solar}\right) dt \tag{3.9}$$

$\dot{S}_{solar}$ denotes the entropy generated from solar energy captured. Entropy is generated by some or all the following processes: friction, mixing, chemical reactions, heat transfer through finite temperature difference, unrestrained expansion, non-quasi equilibrium compression or expansion, etc.

The entropy generated through the process of capturing solar energy could be because of heat transfer through a finite temperature difference. solar entropy can be expressed as

$$\dot{S}_{solar} = \frac{q_{solar}}{T_{sat,1}} \tag{3.10}$$

Exergy provided by solar is then used to raise the temperature of PCM and the total exergy of the system is represented by

$$\Delta Ex_{sys} = \int_{t_0}^{t} \left[m_{PCM} c_{PCM} \frac{dT_{PCM}}{dt} + \rho h_{sl} \frac{dV_l}{dt} + \sum_{i=1}^{5} m_{w,i} c_w \frac{dT_{w,i}}{dt} - T_0 \frac{dS_{sys}}{dt} \right] dt \tag{3.11}$$

where

$$\frac{dS_{sys}}{dt} = m_{PCM} c_{PCM} \frac{dT_{PCM}}{dt} \left(\frac{1}{T_{PCM}} \right) + \rho h_{sl} \frac{dV_l}{dt} \left(\frac{1}{T_m} \right) + \sum_{j=1}^{5} m_{w,j} c_w \frac{dT_{w,j}}{dt} \left(\frac{1}{T_{w,j}} \right) \tag{3.12}$$

and m_{PCM} is calculated as

$$m_{PCM} = \frac{TES_{size} \times 3.6 \times 10^6}{h_{sl}} \tag{3.13}$$

This is the exergy contained in the PCM after exergy destroyed and exergy output.

$$Ex_{out} = \int_{t_0}^{t} \left(q_{water} + q_{air} + q_{AC} - T_0 (\dot{S}_{water} + \dot{S}_{air} + \dot{S}_{AC}) \right) dt \tag{3.14}$$

The PCM properties are analyzed to report the exergy input and output, the exergy changes of the system, entropy generated, and exergy destroyed. In Equation (3.11) and (3.12) T_{PCM} is the PCM temperature averaged over the entire PCM volume. The exergy efficiency over the period is given by:

$$\eta = 1 - \frac{Ex_{des}}{Ex_{in}} \tag{3.15}$$

3.2. Candidate Cities Selection and Equipment Sizing

This section describes the selection process for the candidate cities chosen for this study and the systematic approach to determine the solar collector and LHTES sizes based on the available solar insolation and the building demands.

3.2.1. Candidate city selection

The performance of the LHTES system (expressed using a mathematical model) is weather-dependent. This is because of the difference in weather conditions in different places resulting in a distinction in building loads for heating, cooling, and hot water due to variation of heating degree days, average outdoor temperature, and precipitation. The following are the guidelines to definitions of climate zones obtained from the department of energy website [58]:

1. **Hot-humid:** A hot-humid climate is a region that receives more than 20 in. (50 cm) of annual precipitation and where one or both of the following occur:
    - A 67°F (19.5°C) or higher wet bulb temperature for 3,000 or more hours during the warmest six consecutive months of the year; or
    - A 73°F (23°C) or higher wet bulb temperature for 1,500 or more hours during the warmest six consecutive months of the year.

2. **Mixed-humid:** A mixed-humid climate is a region that receives more than 20 in. (50 cm) of annual precipitation, has approximately 5,400 heating degree days (65°F basis) or fewer, and where the average monthly outdoor temperature drops below 45°F (7°C) during the winter months.
3. **Hot-dry:** A hot-dry climate is a region that receives less than 20 in. (50 cm) of annual precipitation and where the monthly average outdoor temperature remains above 45°F (7°C) throughout the year.
4. **Mixed-dry:** A mixed-dry climate is generally defined as a region that receives less than 20 in. (50 cm) of annual precipitation, has approximately 5,400 heating degree days (65°F basis) or less, and where the average monthly outdoor temperature drops below 45°F (7°C) during the winter months.
5. **Cold:** A cold climate is generally defined as a region with approximately 5,400 heating degree days (65°F basis) or more and fewer than approximately 9,000 heating degree days (65°F basis).
6. **Very cold:** A very cold climate is generally defined as a region with approximately 9,000 heating degree days (65°F basis) or more and fewer than approximately 12,600 heating degree days (65°F basis).
7. **Subarctic:** A subarctic climate is generally defined as a region with approximately 12,600 heating degree days (65° basis) or more.
8. **Marine:** A marine climate is generally defined as a region that meets all the following criteria:

- A mean temperature of the coldest month between 27°F (-3°C) and 65°F (18°C)
- The warmest month mean of less than 72°F (22°C)
- At least 4 months with mean temperatures more than 50°F (10°C)
- A dry season in summer.
- The month with the heaviest precipitation in the cold season has at least three times as much precipitation as the month with the least precipitation in the rest of the year. The cold season is October through March in the Northern Hemisphere and April through September in the Southern Hemisphere.

In this research, seven cities were selected from seven different U.S. climate zones. Shown in Figure 3.3 are the cities that were chosen for this study which are: Miami, FL, from a hot-humid climate zone; Duluth, MN from a very cold climate zone; Oklahoma City, OK from a mixed-humid climate zone; Albuquerque, NM from a mixed-dry climate zone; Los Angeles CA from a hot-dry zone; Reno, NV from a cold climate zone, and Portland, OR from a marine climate zone [59].

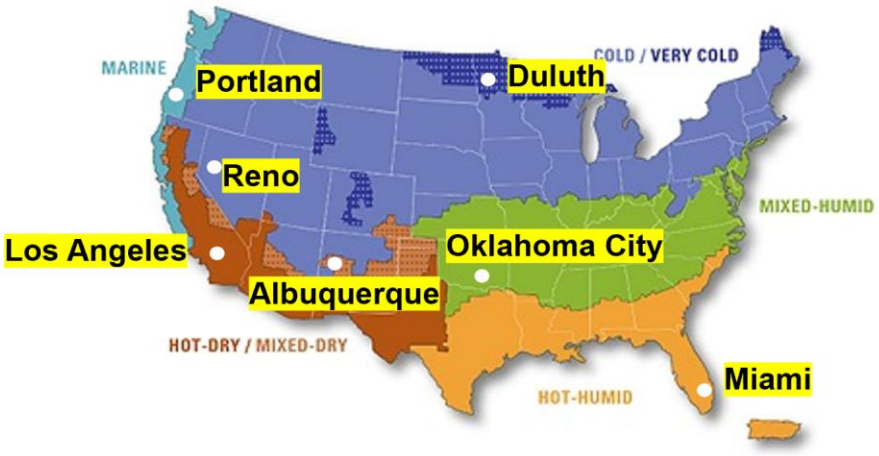

Figure 3.3. Showing ASHRAE Climate Zones and marking selected cities (adopted from [60]*).*

Equipment sizing is determined using the total daily building energy demand for heating, cooling, and hot water loads and solar radiation index. It is desired to meet daily building energy demand; therefore, the solar collector area is sized to supply the total thermal energy required. Solar energy is stored and distributed by the thermal energy storage unit. A step by step details on sizing equipment is discussed in this section.

3.2.2. Daily total energy demand calculation

Hourly data on residential heating, cooling, and hot water loads are available from the OpenEI website [61], affiliated with the U.S. Department of Energy. The daily demand is obtained by adding 24-hour load data for space cooling and heating, and hot water for each day in a TMY

$$Q_d = \int_0^{24} load_h dh \tag{3.16}$$

Throughout this paper, the subscripts d and h represent day and hour, respectively; and $load_t$ is the hourly energy required for heating, cooling, and hot water.

$$load_h = \frac{\mathrm{COP}_{vapor\ compression}}{\mathrm{COP}_{absorption\ chiller}} \times load_{h,cooling} + load_{h,heating} + load_{h,hot\ water} \tag{3.17}$$

$\mathrm{COP}_{vapor\ compression}$ is the coefficient of performance of the vapor compression cycle and is calculated using SEER (seasonal energy efficiency ratio) relations obtained from [62] - [63].

$$SEER = \frac{output\ cooling\ energy\ in\ BTU\ over\ a\ cooling\ season}{input\ electrical\ energy\ in\ Wh\ during\ the\ same\ season} \tag{3.18}$$

The energy efficiency ratio (EER) is the quantity of SEER and can be determined using Equation 3.19.

$$EER = \frac{output\ cooling\ energy\ in\ BTU}{input\ electrical\ energy\ in\ Wh} = 1.12\ SEER - 0.02\ SEER^2 \tag{3.19}$$

Finally, $\mathrm{COP}_{vapor\ compression}$ is calculated using Equation 3.20

$$\mathrm{COP}_{vapor\ compression} = \frac{output\ cooling\ energy}{input\ electrical\ energy}$$
$$= EER\left(\frac{BTU}{wh}\right)\frac{1055\ \left(\frac{J}{BTU}\right)}{3600\ \left(\frac{J}{wh}\right)} = 0.293\ EER \tag{3.20}$$

3.2.3. Solar collector area sizing

The area of the solar collector is determined based on total building energy demand and GHI. The area of the solar collector based on daily energy demand is calculated as

$$A_d = \frac{Q_{d,demand}}{\eta_{collector}\sum_0^{24} GHI} \tag{3.21}$$

GHI is known as the hourly solar radiation index data, which is obtained from the national solar radiation database website reported as the global horizontal index, GHI [64], and $\eta_{collector}$ is the efficiency of the evacuated glass tubed used for solar insolation absorption. The solar collector area averaged over the entire year is given by

$$A_{collector} = {}^{1}/_{365}\sum_{i=1}^{365} A_d \tag{3.22}$$

Therefore, the hourly solar insolation absorbed is calculated as the product of the collector area, GHI, and the efficiency of the solar collector, and is given by [1]

$$Q_{h,solar} = GHI \times A_{collector} \times \eta_{collector} \tag{3.23}$$

3.2.4. Thermal energy storage sizing

The size of thermal energy storage is determined based on excess daily solar energy available and energy demand when solar energy is not available or not sufficient. The excess solar energy is calculated as

$$Q_{d,solar\ excess} = \int_0^{24} \left(\max\left(0, Q_{h,solar} - load_h\right)\right) dh \tag{3.24}$$

The daily energy demand during the times when no solar energy is available is calculated as

$$Q_{d,PCM} = \int_0^{24} \left(\max\left(0, load_h - Q_{h,solar}\right)\right) dh \tag{3.25}$$

Thermal energy stored by the PCM daily is calculated as

$$TES_d = \min(Q_{d,solar\ excess}, Q_{d,PCM}) \tag{3.26}$$

Therefore, the thermal energy storage size TES_{size} is calculated as

$$TES_{size} = {}^{1}/_{365} \sum_{d=1}^{365} TES_d \tag{3.27}$$

3.3. Equipment Base Size

The solar collector area and thermal energy storage sizes were calculated using Excel. The Solar collector efficiency was assumed to be 60%; the SEER value was given as 14 [65]. Equation 3.20 results vapor compression COP of 3.75. The COP of the absorption chiller is approximately one [66].

The solar collector area was calculated using Equation 3.22, and thermal energy storage size was calculated using Equation 3.27. The total annual building energy demand, annual GHI, solar collector area, and thermal energy storage size for the selected cities is presented in Table 3.2.

Table 3.2. Annual total building energy demand, total annual GHI, solar collector area, and thermal energy storage size.

City	Zone	Total annual energy demand (MWh)	Annual GHI (MWh/m^2)	Collector area (m2)	TES_{size} (kWh)
Miami, FL	Hot-humid	15.01	1.72	16.07	14.91
Duluth, MN	Very cold	54.29	1.32	156.67	53.59
Oklahoma City, OK	Mixed-humid	23.63	1.70	39.17	21.54
Albuquerque, NM	Mixed-dry	19.37	2.06	22.71	19.62
Los Angeles, CA	Hot-dry	08.42	1.76	11.04	07.62
Reno, NV	Cold	33.44	1.84	56.40	36.39
Portland, OR	Marine	24.50	1.27	86.28	22.73

The total building load in cold climate zones (i.e., marine and very cold) is relatively high. These climates receive a very low intensity of sunlight, thus larger area of the solar collector, which in turn results in a larger size of thermal energy storage. The same results are reflected in cities in mild climate zones (i.e., cold and mixed humid); however, the equipment sizes in these climates are smaller compared to cold climate zones. On the other hand, the total energy demand is the lowest, and solar radiation intensity is highest in warm climate zones (i.e., mixed dry, hot dry, hot-humid). As a result, the area of the solar collector and the size of thermal energy storage are the smallest of all. In the later chapters of this thesis, the effect equipment size on energy savings and benefits are reported.

4. LHTES SYSTEM HEAT TRANSFER AND ENERGY PERFORMANCE ANALYSIS

As mentioned in Chapter 3, seven cities were selected to study the performance of the LHTES system in different U.S climate zones. First, the heat transfer and exergy analysis are conducted in only one city. Heat transfer and exergy analysis facilitate the understanding of the effect of adjusting the equipment sizes on thermal outlet temperature and the system's exergy efficiency. This effect is common to all the selected cities; thus, only one city was reported to avoid repetition. Second, energy performance analysis and evaluation are conducted on all seven chosen cities. Energy performance analysis and evaluation (i.e., auxiliary energy demand, energy cost analysis, and energy performance evaluation) establishes the feasibility and the benefits of employing the system. In this chapter, the heat transfer and exergy analysis are reported first then, the energy performance analysis and evaluation.

4.1. Heat Transfer and Exergy Analysis

The unit cell has a length of $L = 0.1$ m, and the heat pipes' outer radius is $r_{HP} = 0.015$ m. The condenser section of the input HP and the evaporator section of the output HP is at 110 °C and 80 °C, respectively. The PCM melting temperature is 89°C [67], density is 1550 kg/m^3, the heat of fusion is 162.8 kJ/kg, the thermal conductivity of 0.5 W/m K [68], and specific heat of 554 J/kg K. The PCM is contained within an aluminum metal foam with a porosity of 98% [69]. The

effective thermal conductivity of the PCM-metal foam is calculated using Equation 3.6 and is equal to $k = 2$ W/m K.

The model described in Section 3.1, and 3.2 is programmed using MATLAB and the simulation results related to PCM melt volume fraction (Vf) and temperature at which thermal energy is delivered to the load (T_{PCM}) are evaluated on the first day of every quarter (i.e., Jan 1st, April 1st, July 1st, and October 1st [70]) for a residential building in Los Angeles using different sizes of equipment. In Figure 4.1, the primary and secondary y-axes are used to represent the PCM melt volume fraction and temperature at which thermal energy is delivered to the load, respectively. At first, the model is simulated using equipment size (see details in Section 3.3), then the model is simulated by decreasing and increasing equipment by 50%.

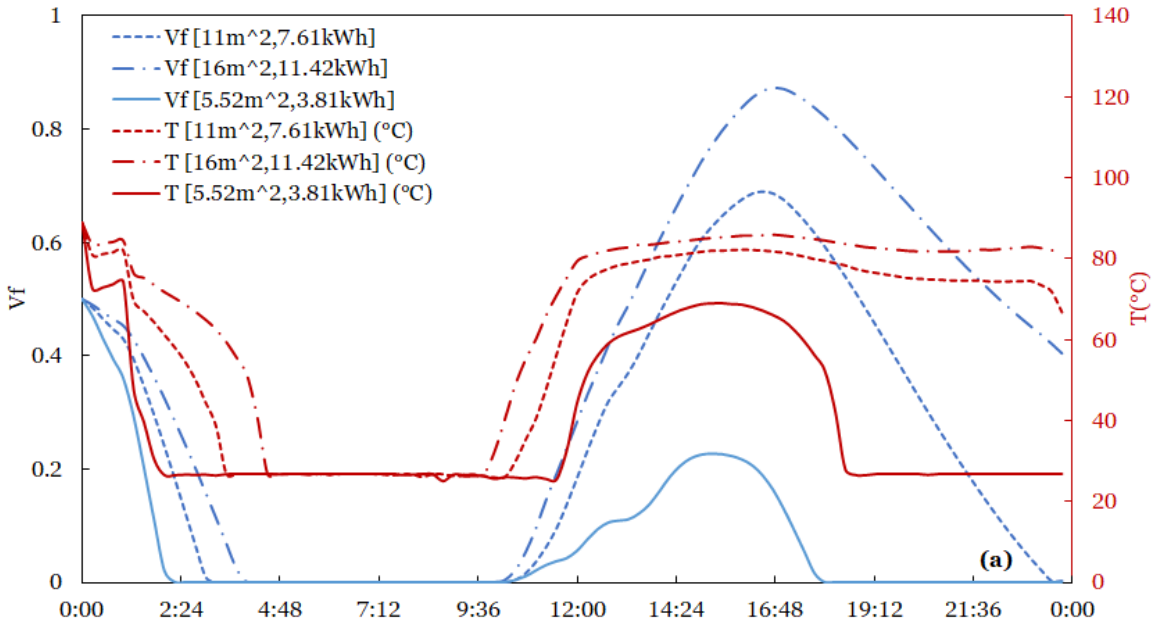

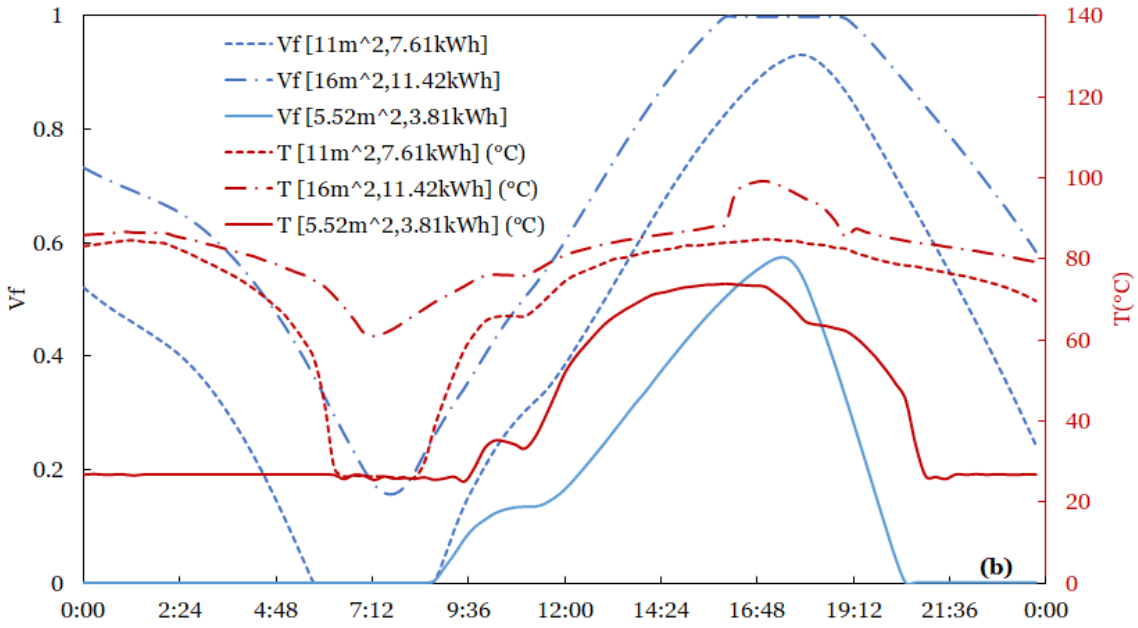
Vf [11m^2,7.61kWh]
Vf [16m^2,11.42kWh]
Vf [5.52m^2,3.81kWh]
T [11m^2,7.61kWh] (°C)
T [16m^2,11.42kWh] (°C)
T [5.52m^2,3.81kWh] (°C)
Vf
T(°C)
0:00
2:24
4:48
7:12
9:36
12:00
14:24
16:48
19:12
21:36
0:00
(b)

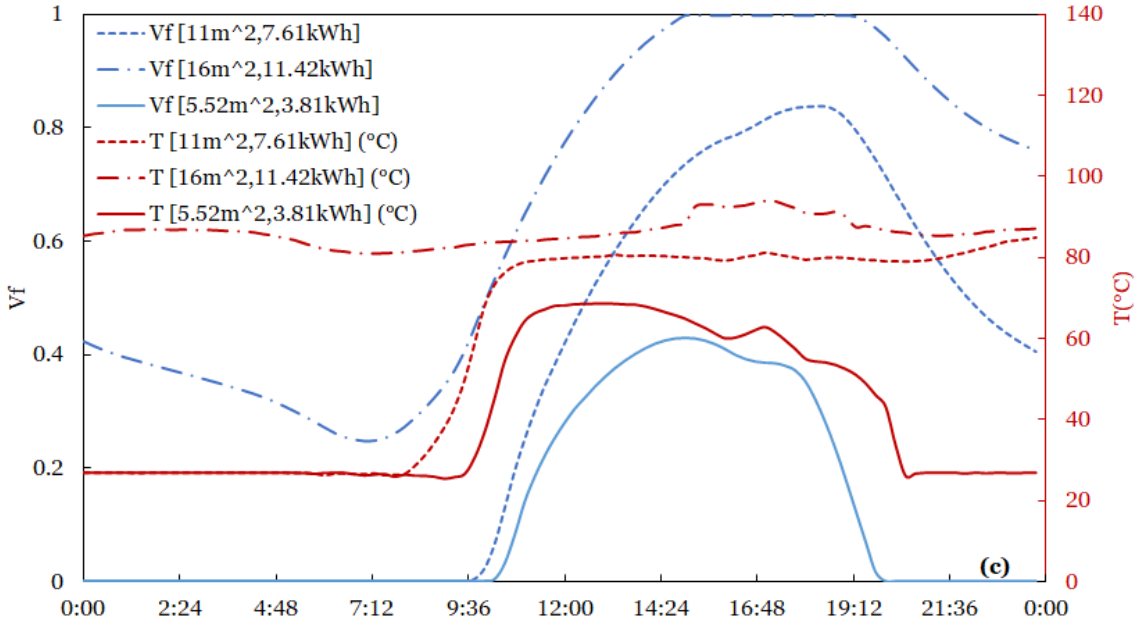
Vf [11m^2,7.61kWh]
Vf [16m^2,11.42kWh]
Vf [5.52m^2,3.81kWh]
T [11m^2,7.61kWh] (°C)
T [16m^2,11.42kWh] (°C)
T [5.52m^2,3.81kWh] (°C)
Vf
T(°C)
0:00
2:24
4:48
7:12
9:36
12:00
14:24
16:48
19:12
21:36
0:00
(c)

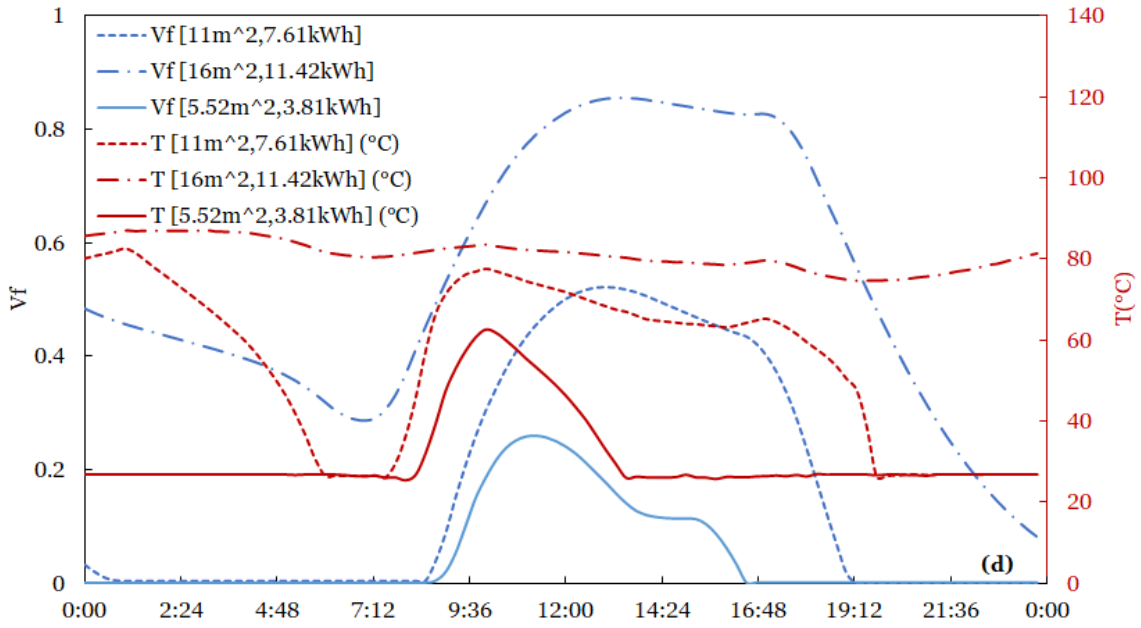

Figure 4.1. Time variation of the melt volume fraction and the temperature at which thermal energy is delivered to the load. (a) Jan 1st, (b)April 1st (c) July 1st and (d) October 1st.

Increasing (decreasing) the solar collector, increases (decreases) the amount of solar energy absorbed by evacuated glass tube solar collector and increasing (decreasing) thermal energy storage results increasing (decreasing) heat transfer surface area, number of the heat pipe and overall PCM volume. Regardless of the amount of thermal energy, the temperature fluctuation in both input and output heat pipes decreases with increasing thermal energy storage size throughout the entire year. On the other hand, the PCM melt volume fraction increases with increasing solar collector area.

Shown in Figure 4.2 is the end of the month exergy efficiency in Los Angeles representing warm climate zone. It is shown that increasing equipment size increases the exergy efficiency of the thermal storage throughout the whole year.

Similar to the temperature, increasing equipment size exergy efficiency of the system due to increased surface area, PCM melt volume, and reduced temperature fluctuation of the system.

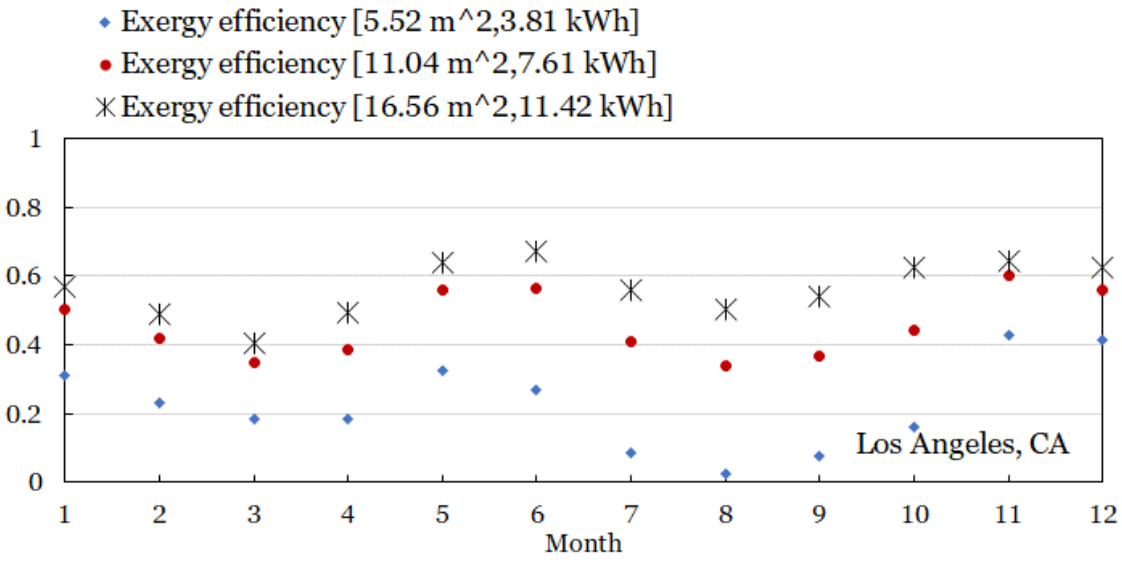

Figure 4.2. End of month exergy efficiency of the latent heat thermal energy storage system in Los Angeles, CA.

4.2. Auxiliary Energy Demand

The auxiliary energy demand is evaluated at both solar collector level (assuming building load is directly supplied by the solar collector) and at the thermal energy storage unit level (by using the LHTES unit to supply the load). The auxiliary energy demand former is termed as energy demand minus solar (Q_{dms}) and energy the auxiliary energy demand at the thermal energy storage level is called auxiliary heater energy demand i.e. (Q_{aux}). The energy demand with a solar collector and no thermal energy storage is calculated as

$$Q_{d,dms} = \int_0^{24} \max\left(0, load_h - Q_{h,solar}\right) dh \qquad (4.1)$$

The subscript d represents a day, and h represents hours. Energy demand with both solar collector and thermal energy storage is calculated as

$$Q_{aux} = \begin{cases} load_h & if\ T_{PCM} \leq 300\ K \\ 0 & Otherwise \end{cases} \qquad (4.2)$$

The lowest allowable discharging PCM temperature occurs at about 300K (26°C). Below this temperature, the auxiliary heater supplies the total energy required for residential building cooling, heating, and hot water loads. When T_{PCM} drops below 300 K, it implies that all PCM solidifies and therefore does not contain sufficient thermal energy. The energy profiles for energy demand with or without solar collectors and thermal energy storage are reported. The results are published city by city in the order: Miami, Duluth, Oklahoma City, Albuquerque, Los Angeles, Reno, and Portland.

4.2.1. Miami, FL

Miami, FL, is in hot-humid climate zones. On average, a residential building in Miami requires a total of 15.01MWh of energy and receives about 1.72MWh/m^2 of solar radiation annually. The simulation results presented in Figure 4.3 was performed using a 16.07 m^2 solar collector coupled with 14.91kWh.

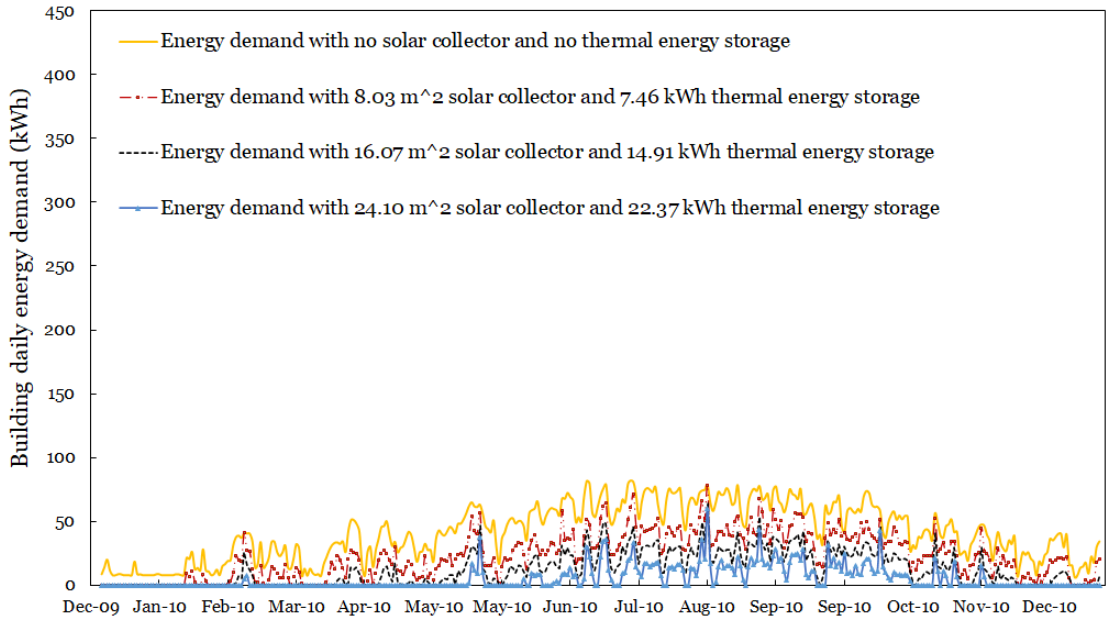

Figure 4.3. Miami - Daily energy demand for residential heating, cooling, and hot water during the typical meteorological year with and without a solar collector.

The gold line is used to represent the energy demand with no solar collector and no thermal energy storage. The crimson long dash-dotted line is used to represent the energy demand with base size minus 50%, the green long dashed line is used to represent energy demand with base size, and the solid blue line is used to represent energy demand with base size plus 50%. The same color coding is used through this chapter in all seven cities. The monthly energy demand is presented in Figure 4.4 using a column chart to display energy demand with only solar collectors and energy demand with both solar collectors and thermal energy

storage.

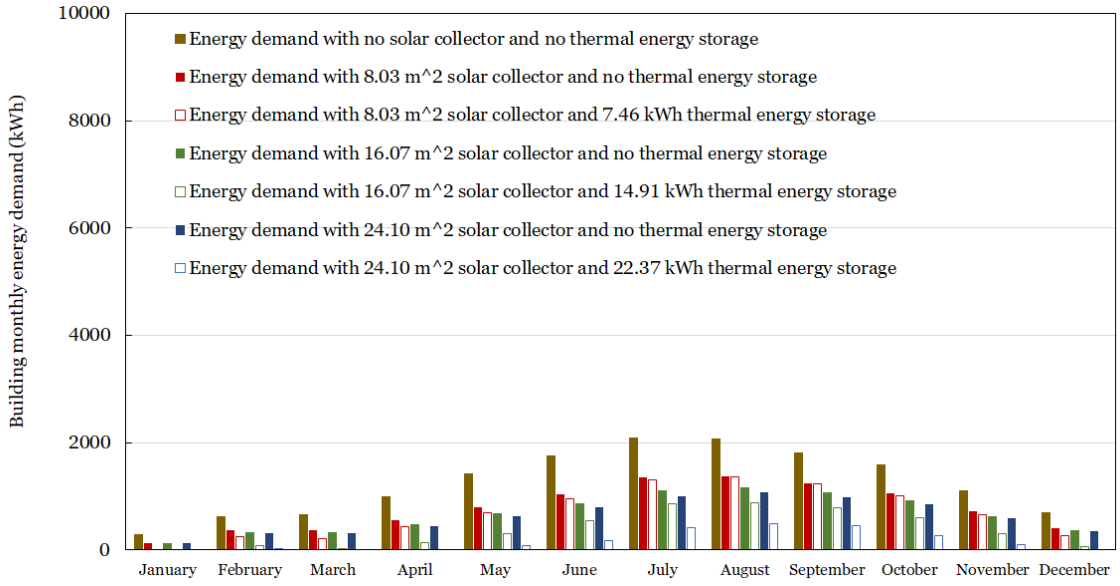

Figure 4.4. Miami - Monthly energy demand for residential heating, cooling, and hot water during the typical meteorological year with and without a solar collector.

The gold bars are used to the monthly energy demand with no solar collector and no thermal energy storage. The green bars are used to represent monthly energy demand with the base size of the equipment. Red bars and blue bars are used to stand for the energy demand with base size minus (add) 50% of the base sizes, respectively. The solid filled bars are used to represent monthly energy demand with only solar collectors, and the empty, filled bars are used to represent energy demand with both solar collectors and thermal energy storage. The same color coding is observed through the rest of the column charts in this chapter.

Generally, increasing the solar collector area reduces energy savings and increasing both solar collectors and thermal energy storage energy savings a lot more. Annually, the energy savings with base sizes, i.e., using a 16.07m^2 solar

collector with no thermal energy storage, yields about a 46% reduction in the annual conventional consumption. Using the same solar thermal collector coupled with a 14.90kWh LHTES unit results in about 69% annual energy saving. Increasing (decreasing) solar collector and thermal energy storage size by 50% increases (decreases) energy saving with the only solar collector to 50% (37%) respectively and by using both solar collector and thermal energy, the energy savings increasing(decreases) to about 86% (44%) respectively.

4.2.2. Duluth, MN

A residential building in Duluth is located in a very cold climate zone. A very cold climate zone is characterized by a region that has more than 9000 heating degree days but less than 12000 (see Section 3.2). A residential building in Duluth requires about 54.29MWh and receives only 1.32MWh/m^2 of solar radiation; thus, a solar collector of about 156.68m^2 and 53.59kWh are required. In Figure 4.5, the daily energy demand with and without solar collector and thermal energy storage for Duluth is presented.

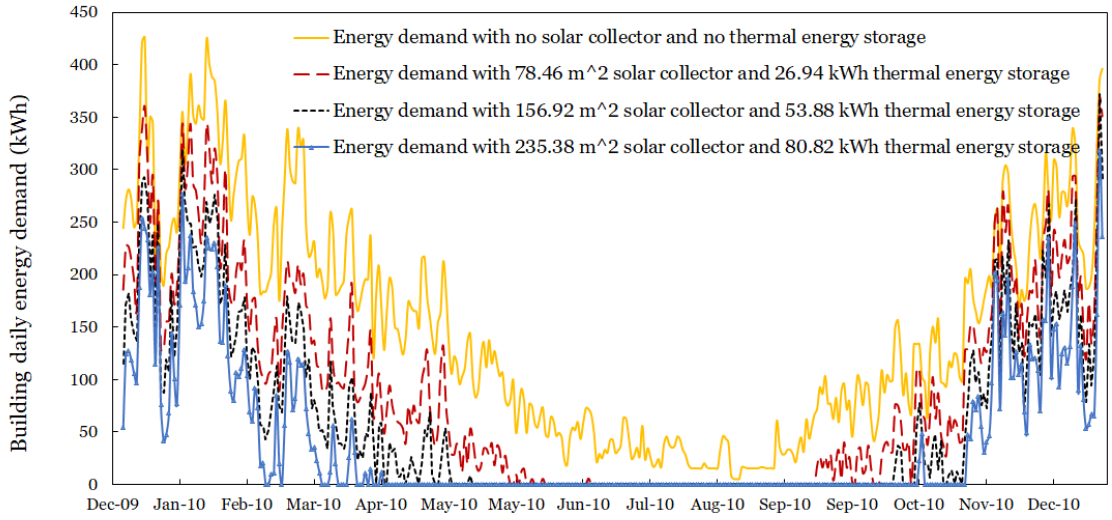

Figure 4.5. Duluth - Daily energy demand for residential heating, cooling, and hot water during the typical meteorological year with and without a solar collector.

In Figure 4.6, a monthly energy demand with and without solar collector and thermal energy storage is reported for a residential building located in Duluth, using a 156.96m^2 solar collector with no thermal energy storage yields about a 36% reduction in the annual conventional consumption. Using the same solar thermal collector coupled with a 53.88kWh LHTES unit results in about 59% annual energy saving. Increasing (decreasing) solar collector and thermal energy storage size by 50% increases(decreases) energy saving with the only solar collector to 38% (30%) respectively and by using both solar collector and thermal energy, the energy savings increasing(decreases) to about 72% (39%) respectively.

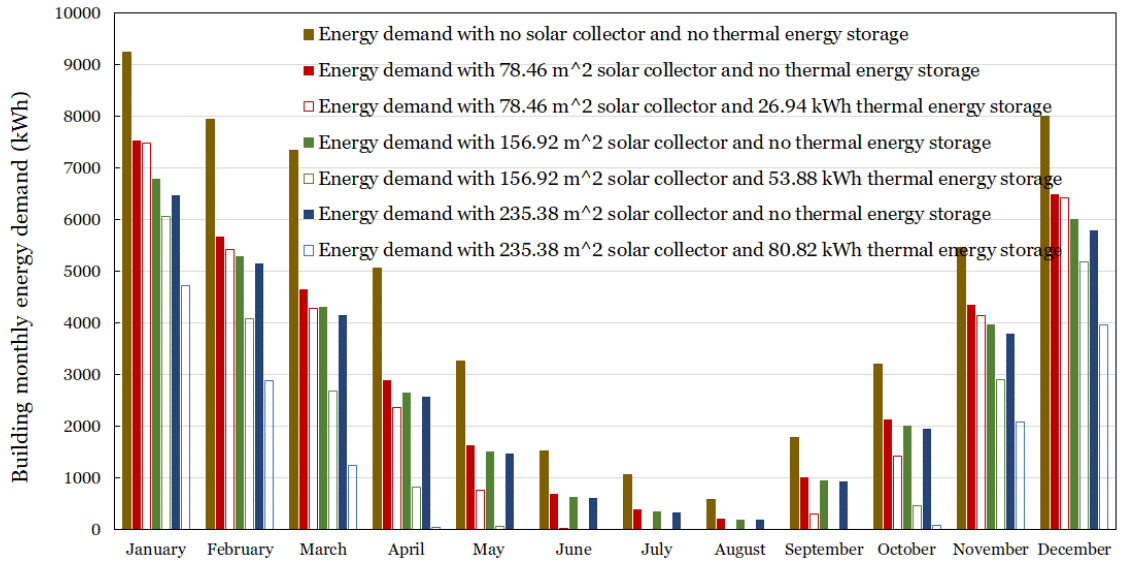

Figure 4.6. Duluth - Monthly energy demand for residential heating, cooling, and hot water during the typical meteorological year with and without a solar collector.

4.2.3. Oklahoma City, OK

A residential building in Oklahoma City experience a mixed-humid climate zone indicating that it receives more than 20 in (50 cm) of annual precipitation and has approximately 5400 heating degree days, and the monthly average outdoor air temperature drops below 45^0F. Generally, a residential building in Oklahoma City requires about 23.63 MWh of energy and the 1.72MWh/m^2 of solar radiation annually; thus, a 39.17m^2 solar collector and 21.59kWh thermal energy storage are required to meet average daily energy demand. The daily building energy demand and reduced energy due to deploying solar collectors and thermal energy storage are shown in Figure 4.7.

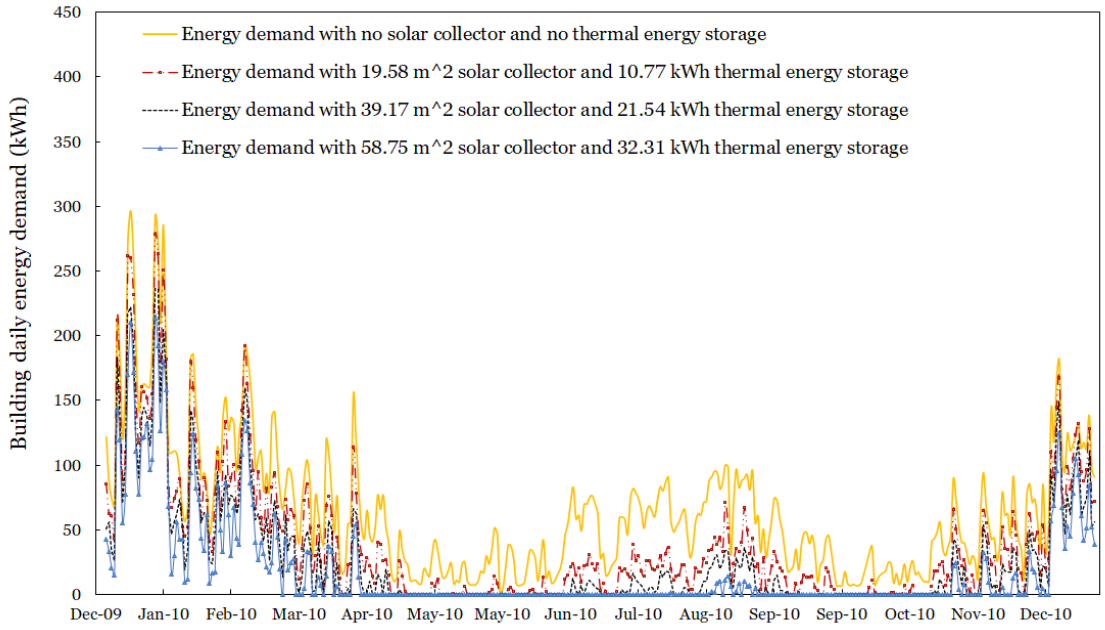

Figure 4.7. Oklahoma City - Daily energy demand for residential heating, cooling, and hot water during the typical meteorological year with and without a solar collector.

A residential building in Oklahoma City, using a 39.17m^2 solar collector with no thermal energy storage yields about 38% reduction in the annual conventional consumption while using the same solar thermal collector coupled with a 21.54kWh LHTES unit results in about 58% annual energy saving (shown in Figure 4.8). Increasing (decreasing) solar collector and thermal energy storage size by 50% increases(decreases) energy saving with the only solar collector to 41% (31%) respectively and by using both solar collector and thermal energy, the energy savings increasing(decreases) to about 71% (39%) respectively.

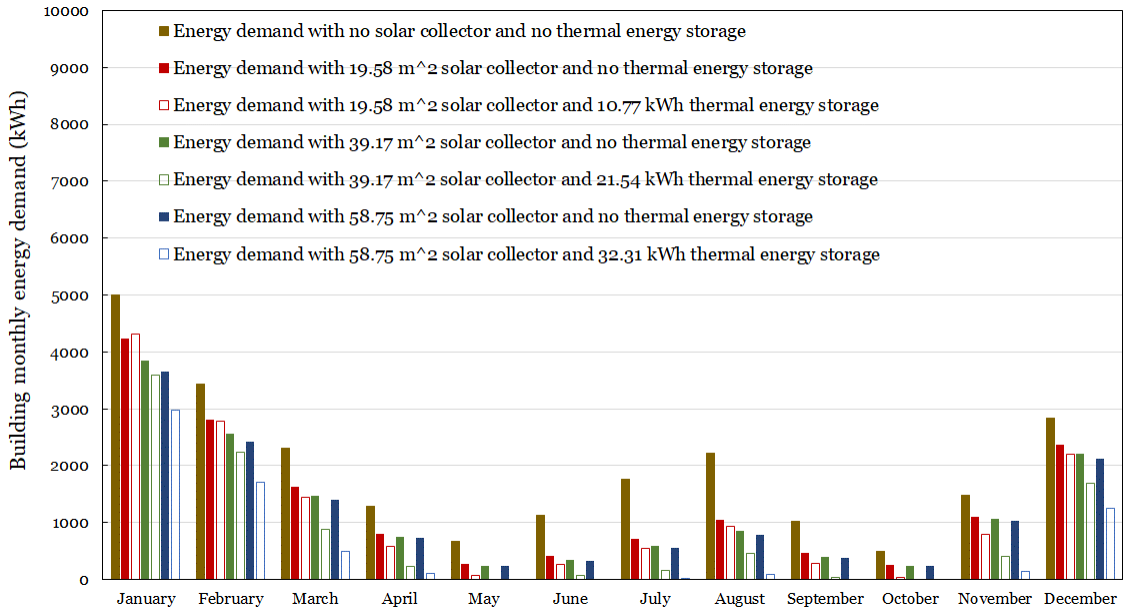

Figure 4.8. Oklahoma City - Monthly energy demand for residential heating, cooling, and hot water during the typical meteorological year with and without a solar collector.

4.2.4. Albuquerque, NM

A residential building in Albuquerque experiences a mixed-dry climate condition. The total energy demand is about 19.37MWh, and about 2.056MWh/m^2 solar radiation is available for harvest. The base equipment sizes are 22.71m^2 collector and 19.62kWh thermal storage. The daily building energy demand and reduced energy due to deploying solar collectors and thermal energy storage are shown in Figure 4.9.

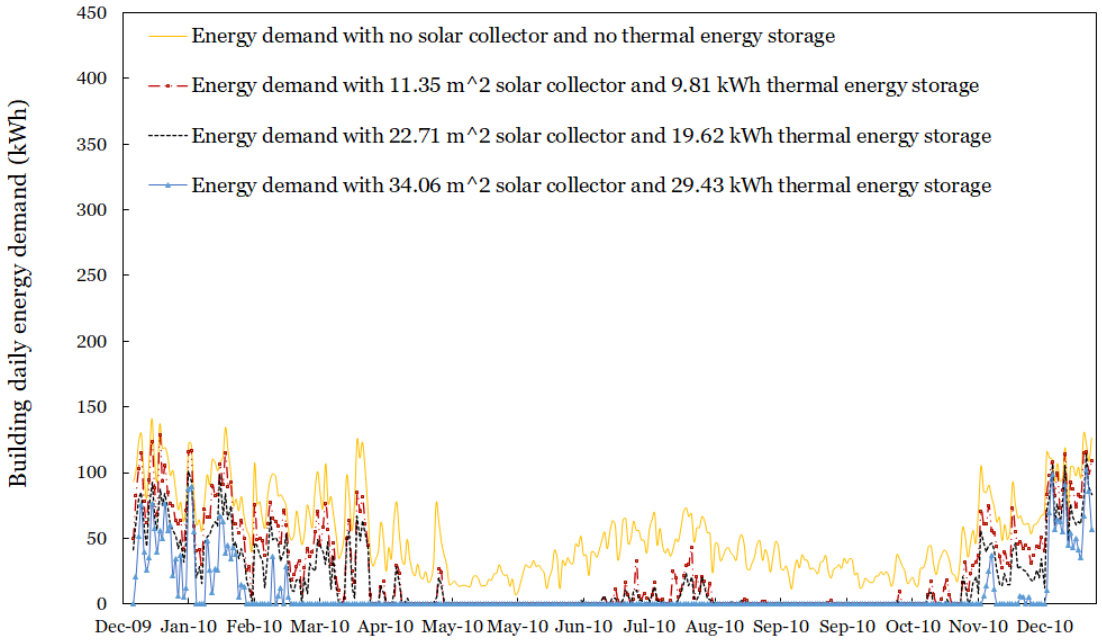

Figure 4.9. Albuquerque - Daily energy demand for residential heating, cooling, and hot water during the typical meteorological year with and without a solar collector.

The monthly energy demands are summarized in Figure 4.10. For a residential building in Albuquerque, using a 22.71m^2 solar collector with no thermal energy storage yields about 38% reduction in the annual conventional consumption. Using the same solar thermal collector coupled with a 19.62kWh LHTES unit results in about 66% annual energy saving. Increasing (decreasing) solar collector and thermal energy storage size by 50% increases(decreases) energy saving with the only solar collector to 40% (30%) respectively and by using both solar collector and thermal energy, the energy savings increasing(decreases) to about 85% (52%) respectively.

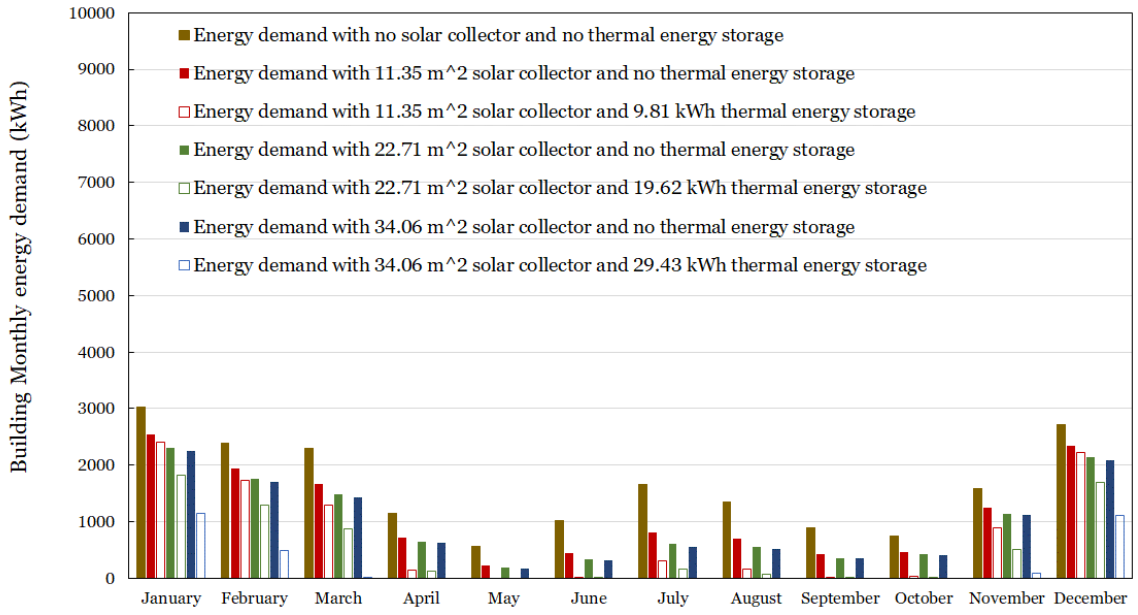

Figure 4.10. Albuquerque - Daily energy demand for residential heating, cooling, and hot water during the typical meteorological year with and without a solar collector.

4.2.5. Los Angeles, CA

A residential building in Los Angeles is in a hot-dry climate zone, i.e., it received less than 20 in (50cm) of annual precipitation, and the monthly outdoor temperature remains above 45 ^{0}F (7^{0}C). The annual energy demand is about 8.418MWh, and the solar radiation index is about 1.76MWh/m^2; thus, 11.04m^2 solar collectors can be used to meet daily energy demand. The thermal energy storage needed is about 7.615kWh. The daily building energy demand and reduced energy due to deploying solar collectors and thermal energy storage are shown in Figure 4.11.

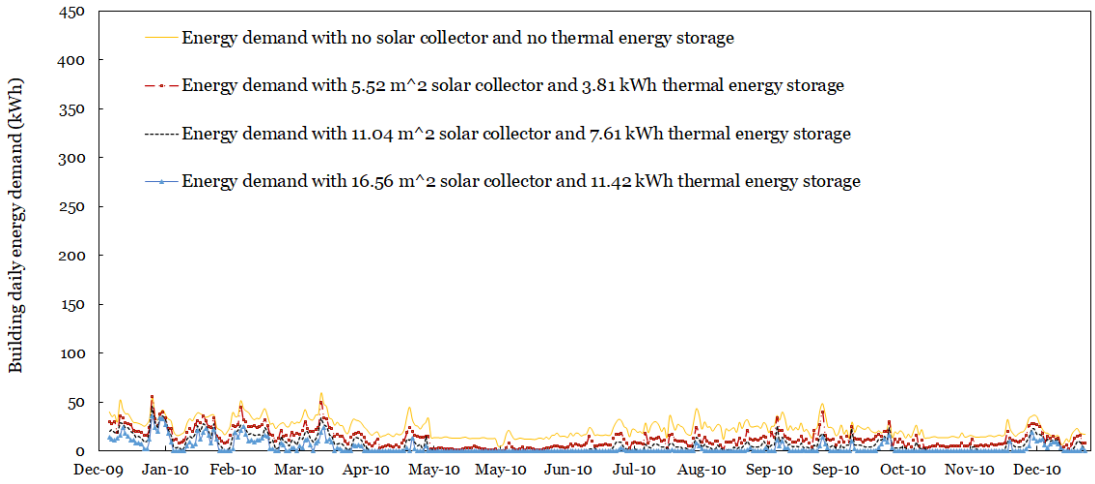

Figure 4.11. Los Angeles - Daily energy demand for residential heating, cooling, and hot water during the typical meteorological year with and without a solar collector.

The monthly energy demand is summarized in Figure 4.12. For a residential building in Los Angeles, using an 11.04m^2 solar collector with no thermal energy storage yields about a 43% reduction in the annual conventional consumption. Using the same solar thermal collector coupled with a 7.61kWh LHTES unit results in about 70% annual energy saving. Increasing (decreasing) solar collector and thermal energy storage size by 50% increases(decreases) energy saving with the only solar collector to 46% (36%) respectively and by using both solar collector and thermal energy, the energy savings increasing(decreases) to about 86% (45%) respectively.

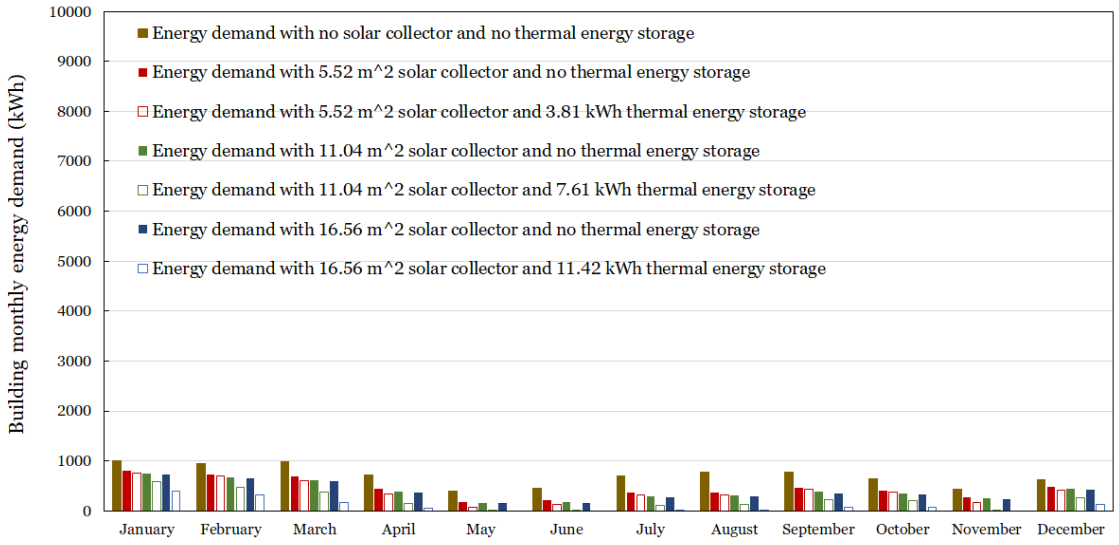

Figure 4.12. Los Angeles - Monthly energy demand for residential heating, cooling, and hot water during the typical meteorological year with and without a solar collector.

4.2.6. Reno, NV

A residential building in Reno experiences a cold climate condition, i.e., heating degree days range between 5400 and 9000. The energy demand to meet heating, cooling, and hot water loads are about 33.437MWh, and the available solar radiation is 1.84MWh/m^2. A 56.4 m^2 solar collector and 36.39kWh thermal energy storage are required as base sizes. The daily building energy demand and reduced energy due to deploying solar collectors and thermal energy storage are shown in Figure 4.13.

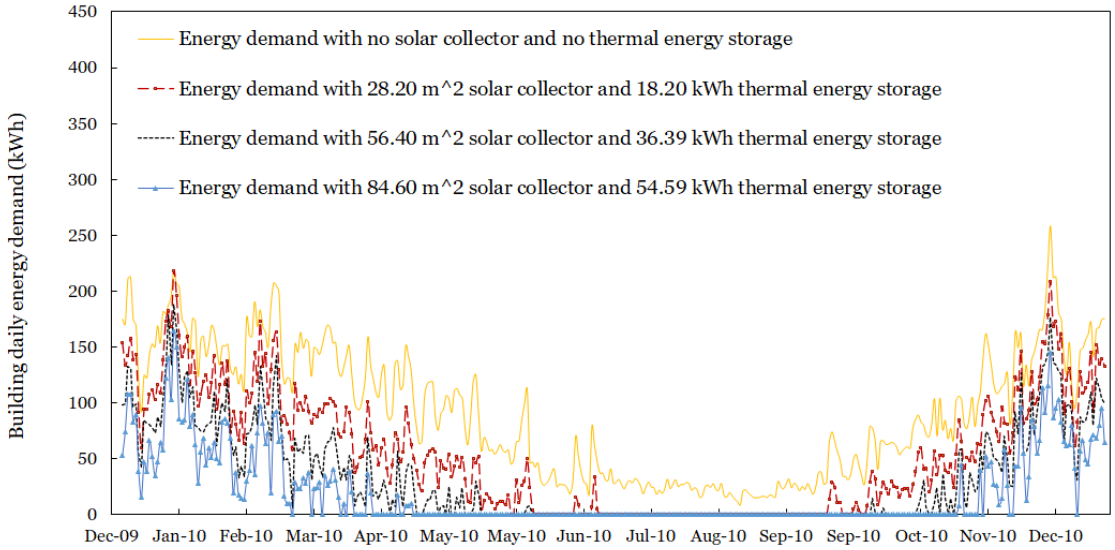

Figure 4.13. Reno - Daily energy demand for residential heating, cooling, and hot water during the typical meteorological year with and without a solar collector.

In Figure 4.14, a monthly energy demand with and without a solar collector is presented. For a residential building in Reno, using a 28.20 m^2 solar collector with no thermal energy storage yields about a 34% reduction in the annual conventional consumption. Using the same solar thermal collector coupled with a 36.39kWh LHTES unit results in about 63% annual energy saving. Increasing (decreasing) solar collector and thermal energy storage size by 50% increases(decreases) energy saving with the only solar collector to 36% (28%) respectively and by using both solar collector and thermal energy, the energy savings increasing(decreases) to about 78% (42%) respectively.

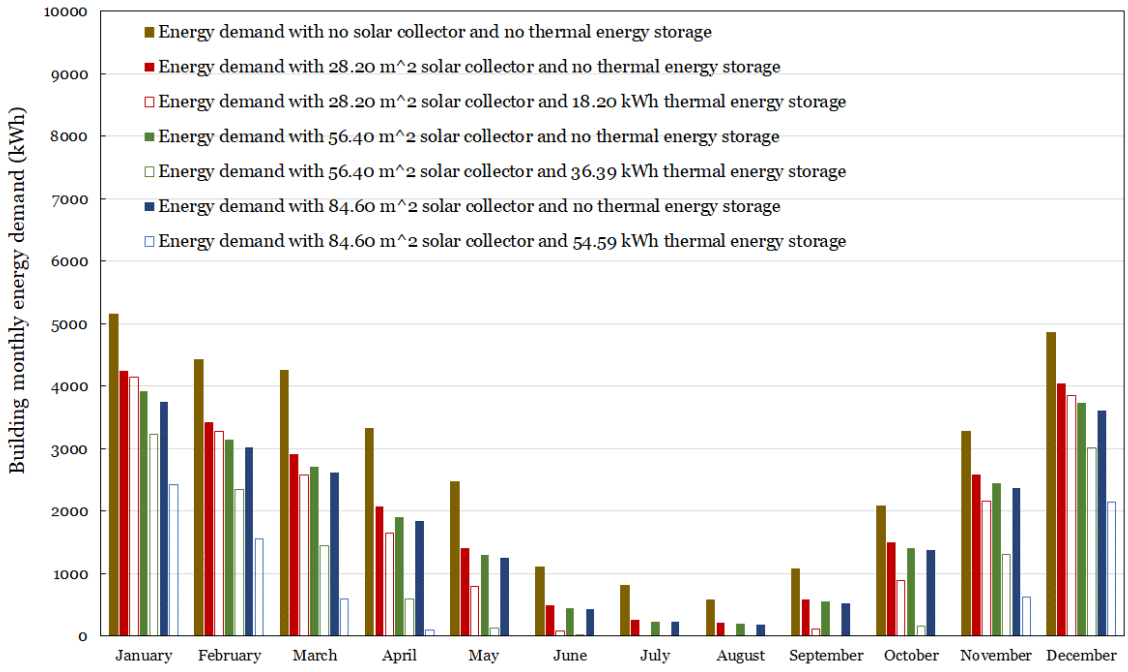

Figure 4.14. Reno - Monthly energy demand for residential heating, cooling, and hot water during the typical meteorological year with and without a solar collector.

4.2.7. Portland, OR

A residential building in Portland experiences a marine climate condition. The energy demand to meet heating, cooling, and hot water loads are about 24.50 MWh, and the available solar radiation is 1.27MWh/m^2. A solar collector of 86.28m^2 coupled with a 22.73kWh thermal energy storage is required as base sizes. In Figure 4.15, daily energy with and without solar collector are presented. The daily building energy demand and reduced energy due to deploying solar collectors and thermal energy storage.

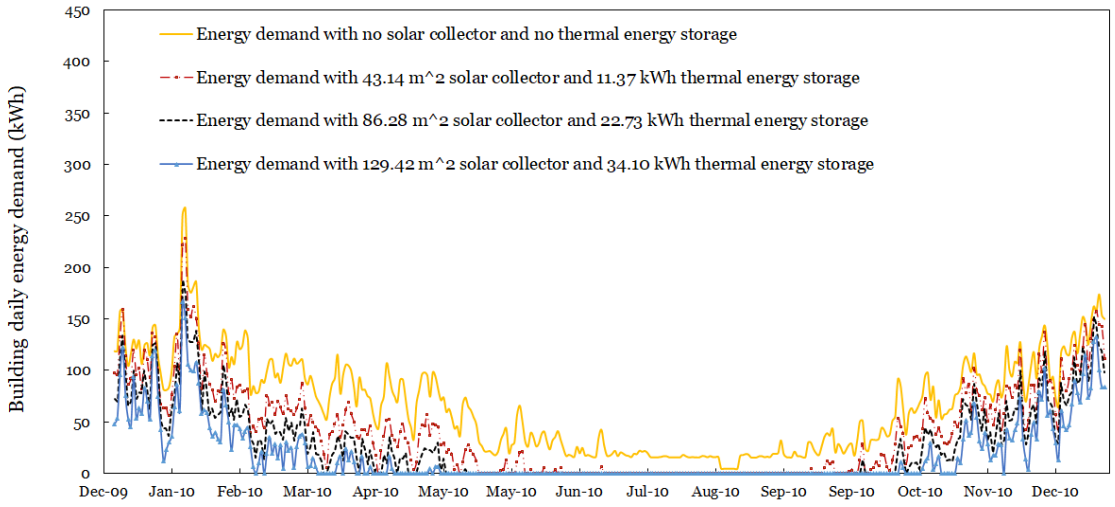

Figure 4.15. Portland - Daily energy demand for residential heating, cooling, and hot water during the typical meteorological year with and without a solar collector.

In Figure 4.16, a monthly energy demand with and without a solar collector is presented. For a residential building in Portland, using 86.28m^2 solar collectors with no thermal energy storage yields about 37% reduction in the annual conventional consumption. Using the same solar thermal collector coupled with a 22.73kWh LHTES unit results in about 58% annual energy saving. Increasing (decreasing) solar collector and thermal energy storage size by 50% increases(decreases) energy saving with the only solar collector to 40% (31%) respectively and by using both solar collector and thermal energy, the energy savings increasing(decreases) to about 72% (40%) respectively.

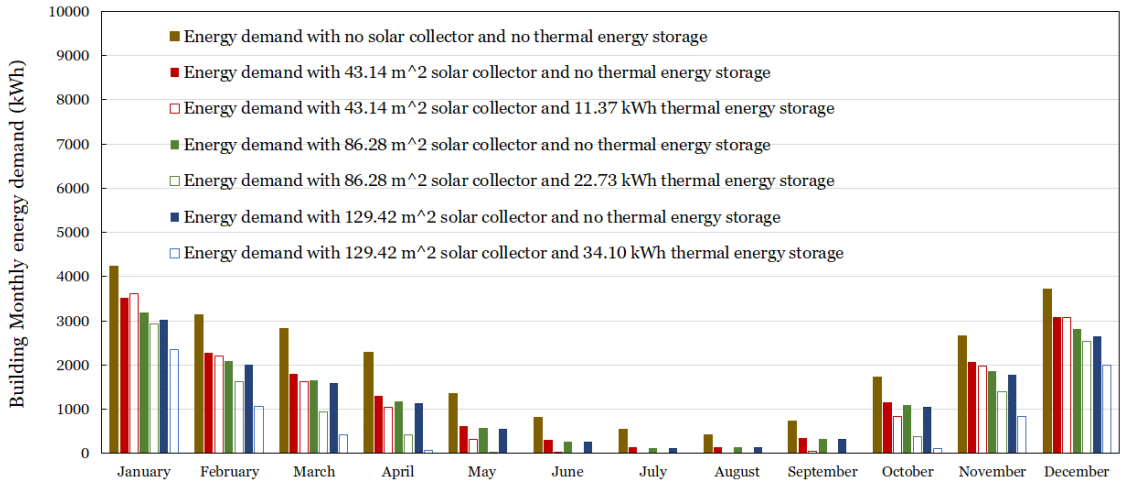

Figure 4.16. Portland - Monthly energy demand for residential heating, cooling, and hot water during the typical meteorological year with and without a solar collector.

4.3. Energy Cost Analysis

The energy cost was evaluated using the residential utility rates listed in Table 4.1. The utility rate is obtained from the U.S energy information administration website [71]. Natural gas price is provided in $/Mcf (dollar per thousand cubic feet). The following conversion was implemented to obtain natural gas price in $/kWh (dollar per kilowatt-hour) [72]:

- Electricity: 1 kW = 3,413 Btu/hr
- Natural gas: 1 MCF = 1,000 cu ft = 10 therms = 1,034,000 Btu = 1.034 MMBtu

Table 4.1 Utility rate for the candidate cities

	Natural gas		Electricity
	$/Mcf	$/kWh	$/kWh
Miami	17.89	0.059	0.106
Duluth	08.76	0.029	0.084
Oklahoma City	11.12	0.037	0.076
Albuquerque	09.63	0.032	0.084
Los Angeles	09.92	0.033	0.130
Reno	12.25	0.040	0.097
Portland	12.49	0.041	0.076

Presented in Table 4.2 is the auxiliary energy cost, the total building energy cost for the candidate cities using different equipment sizes. The table records the annual building energy consumption with and without solar collectors as well.

Table 4.2 The annual energy cost savings

City	TES (kWh)	Collector area (m^2)	Annual total energy demand (kWh)	Total energy demand cost ($)	Auxiliary energy demand (kWh)	Auxiliary energy cost ($)
Miami, FL	07.46	08.04	15010.49	494.87	8353.17	493.26
	14.91	16.07			4538.63	268.01
	22.37	24.11			1976.71	116.73
Duluth, MN	26.94	78.46	54288.39	1568.41	32591.49	942.38
	53.88	156.92			22228.05	642.72
	80.82	235.38			14979.55	433.13
Oklahoma City, OK	10.77	19.59	23632.19	770.99	14250.17	523.05
	21.54	39.17			9761.62	358.30
	32.31	58.76			6782.26	248.94
Albuquerque, NM	09.81	11.36	19370.82	579.32	9213.49	292.86
	19.62	22.71			6572.86	208.93
	29.43	34.07			2853.49	90.70
Los Angeles, CA	03.81	05.52	8417.77	278.78	4655.95	152.45
	07.61	11.04			2473.08	80.98
	11.42	16.56			1217.47	39.86
Reno, NV	18.195	28.200	33437.25	1344.33	19558.15	790.82
	36.39	56.40			12234.57	494.70
	54.59	84.60			7453.70	301.39
Portland, OR	11.37	43.14	24498.81	1010.00	14782.37	609.43
	22.73	86.28			10261.98	423.07
	34.10	129.42			6854.15	282.57

The energy cost and energy saving in the residential building make up a huge role in determining the benefits of the LHTES system in residential buildings. Energy savings not only depends on the size of the equipment utilized but also on the rate at which energy is supplied and drawn from the thermal energy storage unit.

First, examining the energy cost and saving by size, larger sizes result in higher energy savings in all the seven climate zone; therefore, larger equipment size can contribute to higher energy cost savings. However, larger equipment size can result in higher equipment costs (equipment cost analysis is beyond the scope of this study, thus left out for the next phase of research).

Second, the rate at which solar energy is supplied to and drawn from the system emulates better energy savings. For example, a residential building in warmer climate zones such as the hot, dry climate of Los Angeles experiences a vast amount of solar energy through the year, thus grant the constant supply of thermal energy required to meet the building energy demand throughout the year. In that regard, a quite large amount of energy reduction is observed, leading to a significant cut in energy cost annually. On the other hand, a building located in Duluth experiences a long winter period with insufficiency or no solar energy, thus fewer energy savings. The reduced energy saving could be reversed by increasing the size, which results in a non-economic system.

4.4. Energy Performance Evaluation

The energy performance evaluation indices, i.e., solar utilization index, annual saving per unit PCM mass, and annual energy saving results in a guide to selecting the optimal size of the equipment by determining the energy benefit of deploying the LHTES system in different climate zones. The energy evaluation indices employed are:

1. The annual energy savings per unit mass of thermal energy storage (α_{spm}) is calculated as

$$\alpha_{spm} = \frac{Q_{annual,demand} - Q_{annual,aux}}{m_{PCM}} \tag{4.3}$$

2. The annual energy savings per unit area (α_{spa}) is evaluated as

$$\alpha_{spa} = \frac{Q_{annual,demand} - Q_{annual,aux}}{A_{collector}} \tag{4.4}$$

3. The solar energy utilization ratio is evaluated as (β_{solar})

$$\beta_{solar} = \frac{Q_{annual,demand} - Q_{annual,aux}}{Q_{annual,solar}} \tag{4.5}$$

Energy performance evaluation indices were calculated using Excel. In Figure 4.17, α_{spm} versus α_{spa} are plotted. The black long dashed-dotted circles enclose the results obtained using equipment base size (see Table 3.2). Solid blue and red dashed circles are using to enclose the results obtained by decreasing and increasing the equipment base size by 50%, respectively. As such, three sets of results are identified, and each set contains three groups. Set 1 is marked with a numeric with no subscript, Set 2 is marked with a numeric and minus (-) subscript and Set 3 with a numeric and a plus (+) sign.

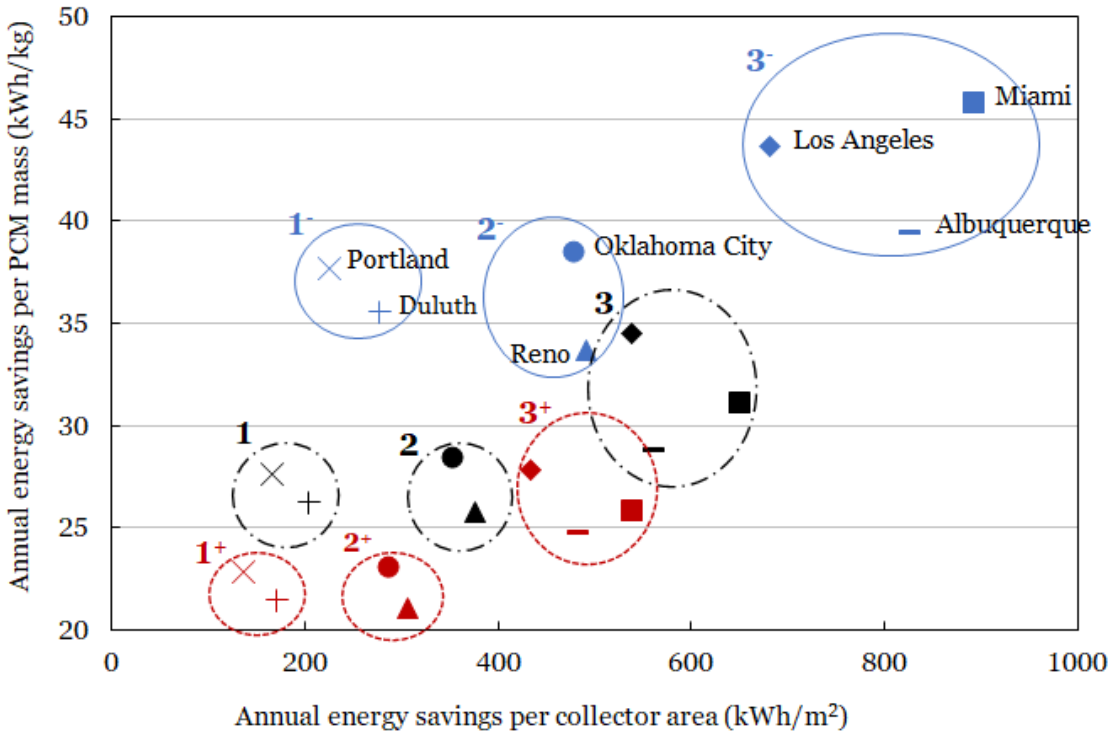

Figure 4.17. Energy savings per collector size versus energy saving per PCM mass.

Set 1 Group 1 constitutes residential buildings from cities in cold climate zones (i.e., Portland and Duluth) results using equipment base size. These cities reflect the largest equipment sizes compared to the rest of the cities. The larger equipment sizes are due to high energy heating, cooling, and hot water energy demand, and low solar radiation. Cities in this group have the smallest energy saving per unit PCM mass and energy savings per unit area. The solar utilization ratios, using base sizes, are 0.21 and 0.25 for Portland and Duluth, indicating that about 80% and 85% of absorbed solar is not used to supply heating, cooling, and hot water energy demand. Decreasing (increasing) equipment size by 50%, results Set 1^- (Set 1^+), reduces (increases) how much solar energy captured and distributed

in the system. Less (more) than needed solar energy is captured, leading to increased (decreased) solar utilization ratio. In Figure 4.18, Daily total building energy and the absorbed solar energy for Duluth, Oklahoma City, and Los Angeles (scaled for better visualization) are presented. Note that, three cities are displayed each to represent each group from which it belongs (shown in Figure 4.17)

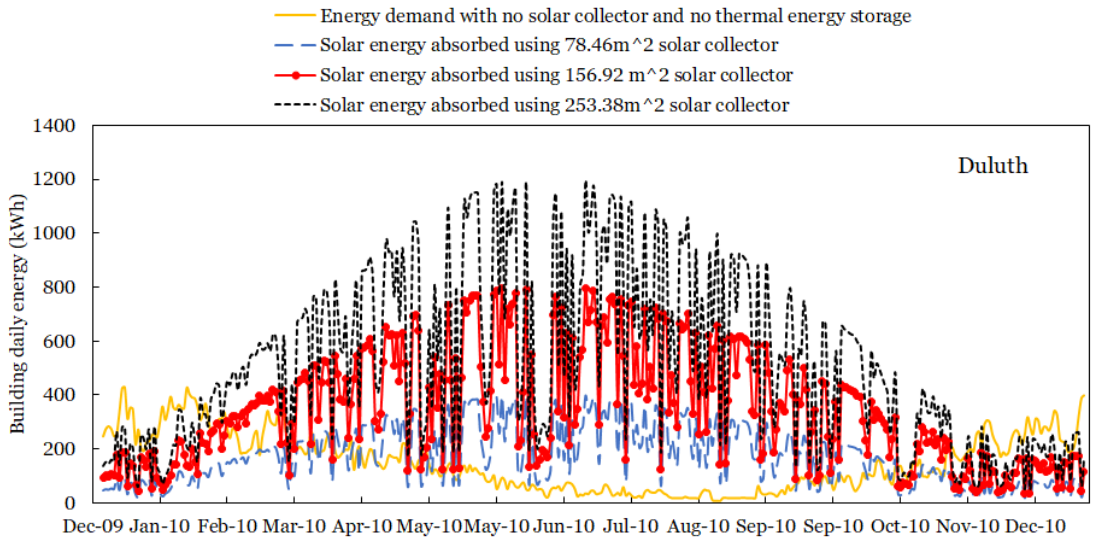

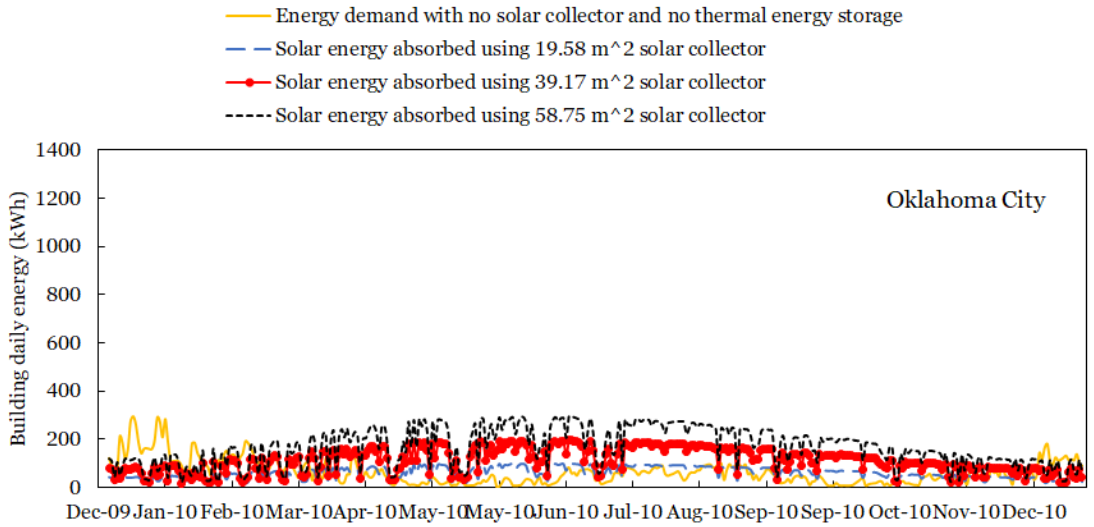

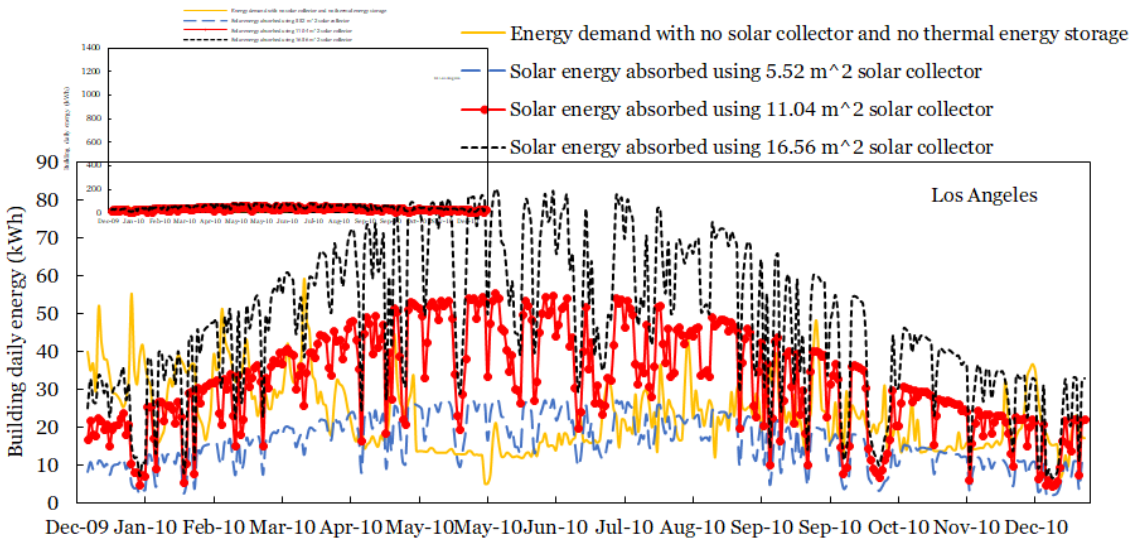

Figure 4.18. Daily total building energy and the absorbed solar energy (1) Duluth, (2) Oklahoma City, and (3) Los Angeles

A larger solar collector of 156.92m^2 absorbed much higher solar energy than needed (especially in February through November), leading to a lower solar utilization ratio. The same results are observed in all the three presented and the rest of the cities, thus not shown here (presented in Appendix). The solar utilization decreases (increases) upon increasing (decreasing) equipment sizes (especially solar collector). The resulting solar utilization is 0.35 (0.21) for Duluth and 0.30 (0.17) for Portland at decreasing (increasing) equipment size. As a result, it is not beneficial to run the LHTES system in colder climate zones. It is noted from 4.18 that the equipment is oversized (for Duluth and Portland), leading to the smallest solar utilization ratios. Upon completing equipment and installation cost and experimentation (which are beyond the scope of this thesis), the decision to deploy or not to deploy the LHTES system in colder climate zones could be strengthened.

Group 2 consists of residential buildings in cities belonging to mild climate zones, i.e., Oklahoma City and Reno. The solar utilization ratios are moderate. For example, using base sizes, the solar utilization ratio for Oklahoma City and Reno are 0.35 and 0.34, respectively. The equipment sizes for Oklahoma City are much smaller compared to that of Reno; thus, the energy benefit is better in Oklahoma City than in Reno. Decreasing (increasing) equipment base size results in an increased (decreased) solar utilization. The resulting solar utilization ratio is increased (decreases) to 0.47 (0.28) and 0.43 (0.28) for Oklahoma City and Reno, respectively. It is recommended to deploy the LHTES system in these two cities using the smallest possible equipment sizes (i.e., 50% of equipment base size) because they reflect a better solar utilization ratio. Like mentioned for Group 1, capital cost should be assessed first before deciding the deployment.

Group 3 is composed of cities from warmer climate zone, i.e., Miami from hot-humid, Albuquerque from mixed-dry, and Los Angeles from hot-dry. The energy savings per unit PCM mass and energy savings per unit area reflect the highest among all the groups. Considering the base size, the solar utilization ratio is 0.63, 0.51, and 0.46 for Miami, Albuquerque, and Los Angeles, respectively. Decreasing (increasing) equipment sizes increases (decreases) energy savings per solar utilization ratio to 0.80 (0.52), 0.73 (0.39) and 0.64 (0.41) for Miami, Albuquerque and Los Angeles respectively. It is recommended employing equipment with base sizes for cities belong to this group.

Generally, decreasing the equipment sizes increases the energy benefit in all the cities and all in about the same range. In the Warmer climate zone, the energy benefit is smaller than in colder climate zones. In warmer climate zones such as hot-dry (Los Angeles), hot-humid (Miami) and Mixed-humid, decreasing (increasing) the equipment base size increases (decreases) both the annual energy savings per collector area and energy savings per PCM mass by 1.27 (0.80), 1.27 (0.83), and 1.59(0.86) respectively. Decreasing (increasing) equipment size in Mild and cold climate zones such as mixed-humid (Oklahoma City), cold (Reno), very cold (Duluth) and marine (Portland) increases (decreases) equipment base size increases (decreases) both the annual energy savings per collector area and energy savings per PCM mass by 1.35 (0.80), 1.31 (0.82), 1.37 (0.83), and 1.35 (0.82) respectively.

5. CLOSING REMARKS

In this thesis, state of the art in modeling, simulation of heating, cooling, and hot water system integrated with latent heat thermal energy storage in residential buildings was reviewed. Next, a thermal network heat transfer model was employed to quantify the energy performance of the solar HVAC and hot water system integrated with LHTES for residential applications. The model was extended for continuous annual energy analysis of the system. The extended model was employed to investigate the potential of the present system in decreasing the building energy costs in various climate zones. In the end, an energy performance analysis resulted in a report on energy saving, energy cost analysis, and the system benefits evaluation. The main findings of this study are summarized in the following:

1. The extensive literature review has revealed the existence of integration of LHTES thermal energy storage with only space heating, space cooling, hot water system, heat pump, absorption air condition unit or the combination of two different units and no study has put all the three together, i.e., cooling, heating, and hot water system. Further, the existing research of an integrated system simulates the heat transfer and exergy of the system for a cold day and a hot day thus no current study that adds building heating, cooling, and hot water loads to heat transfer and exergy model and simulate for the entire year (i.e., 365 days). As a result, blending in the building load and simulating the

model for the whole year sets in the innovation approach and is the focal point of this study.

2. Investigation and selection of the candidate cities have exposed the distinction of climate zones owed to the difference in the amount of solar energy, heating, cooling, and hot water loads due to different heating degree days, annual precipitation, and average monthly outdoor temperature. As the results of the existing distinctions, the equipment sizes required differ from one climate zone to another. Hence, warmer climate zones need smaller equipment sizes, and colder climate zones require larger equipment sizes.
3. Adjusting the equipment sizes establishes a knowledge base on the outcome of heat transfer, exergy efficiency, energy savings, and energy cost savings. The heat transfer improves upon increasing the equipment sizes due to increased heat transfer areas that lead to reduced temperature fluctuation in both input and output sections of the heat pipe. Further, solar energy supply increases the rate of PCM melting and avails more energy provision to meet the building energy demand. As a result, the exergy efficiency improves significantly. The availability of more solar energy upsurges the energy savings and scales down energy costs in all the seven climate zones.
4. It is shown that the LHTES system can reduce the auxiliary energy input needed to meet the demands of a residential building located in all seven climate zones; however, it is more beneficial in warmer climate zones than in colder climate zones. In warmer climate zones, the equipment sizes are smaller,

the annual energy savings per unit mass of thermal energy storage is larger, and the annual solar energy utilization ratio is higher, indicating that the LHTES system is more beneficial in the warmer climate zones (cities), i.e., hot humid (Miami); mixed-dry (Albuquerque); and hot dry (Los Angeles) than in colder climate zones (cities), i.e., very cold (Duluth); mixed-humid (Oklahoma City); cold (Reno); and marine (Portland).

Energy performance evaluation sets up the knowledge base on the benefit of deploying the system in different U.S climate zones. Generally, the energy savings percentage, cost savings, saving per unit area of solar collector, saving per unit mass of LHTES unit, and solar utilization ratio are high in warmer climate zones, low in mild climate zones and lowest in cold climate zone indicating that it is more beneficial to employ LHTES system in warmer climate zones such as hot-humid, hot dry and mixed dry than in mild climate zones (such as mixed humid and cold) and cold climate zones (such as very cold and marine). This is because of increased equipment sizes, which would result in increased capital cost, thus less beneficial for employing the system in such climate zones.

In conclusion, this study provides a knowledge base on modeling, simulation, and energy performance evaluation in a residential building with heating, cooling, and hot water systems integrated with latent heat thermal energy storage and sustains the decision to deploy the LHTES system in the HVAC industry. Thermal energy storage (TES) systems grant both environmental and economic benefits by reducing the need for burning fuels and depletion of other

non-renewable energies. Thermal energy storage (TES) systems prevent the loss of thermal energy by storing excess heat until it is consumed. Almost in every human activity, heat is produced. Our actions in the kitchen, automobile, etc., when seen at a macro scale, collectively generate a vast amount of heat, which gets wasted all the time. An economical way to store thermal energy from various heat energy sources such as solar thermal energy, geothermal energy, fossil–fuel power plants, nuclear power plant, industrial waste heat could potentially conserve energy and environment at a large scale [73].

The future work should revolve around the following:

1. **Experimentation**. The work presented in this thesis based on theoretical modeling, simulation, and evaluation. There is a need for experimentation aiming at the validation of the theoretical models and provision of firm ground in deploying the LHTES system in buildings or other sectors.
2. **Investigation of the capital cost**. A study on the equipment cost and installation should be thoroughly conducted to determine the affordability of the LHTES system. The monetary factors can potentially stir the deployment of the system in residential buildings or other sectors/industries.

REFERENCES

[1] Shabgard H, Song L, Zhu W. Heat transfer and exergy analysis of a novel solar-powered integrated heating, cooling, and hot water system with latent heat thermal energy storage. Energy Conversion and Management. 2018;

[2] Evacuated Tube Solar Collectors | Apricus Eco-Energy [Internet]. [2020 Jun 3]. Available from: https://www.apricus.com/Evacuated-Tube-Solar-Collectors-pl3681275.html

[3] Evacuated Tube Collectors — Solar Tribune [Internet]. [2020 Jun 3]. Available from: https://solartribune.com/evacuated-tube-solar-hot-water/

[4] Papadimitratos A, Sobhansarbandi S, Pozdin V, Zakhidov A, Hassanipour F. Evacuated tube solar collectors integrated with phase change materials. Solar Energy. 2016;129:10–9. Available from: http://dx.doi.org/10.1016/j.solener.2015.12.040

[5] Demirbas MF. Thermal Energy Storage and Phase Change Materials: An Overview. Energy Sources, Part B: Economics, Planning, and Policy. 2006 Jan 1 [2020 Jun 1];1(1):85–95. Available from: http://www.tandfonline.com/doi/abs/10.1080/009083190881481

[6] Hong ST, Herling DR. Open-cell aluminum foams filled with phase change materials as compact heat sinks. Scripta Materialia. 2006 Nov;55(10):887–90.

[7] Rosenberg M. Analyzing Air Handling Unit Efficiency [Internet]. [2020 Jul 14]. Available from: www.onsetcomp.com

[8] Hossain MS, Saidur R, Fayaz H, Rahim NA, Islam MR, Ahamed JU, et al. Review on solar water heater collector and thermal energy performance of circulating pipe. Vol. 15, Renewable and Sustainable Energy Reviews. Pergamon; 2011. p. 3801–12.

[9] Hayter SJ, Kandt A, Kandt F-A. Renewable Energy Applications for Existing Buildings Preprint Renewable Energy Applications for Existing Buildings Applicazioni dell'energia rinnovabile su edifici esistenti [Internet]. 2011 [2020 May 31]. Available from: http://www.osti.gov/bridge

[10] Solar Energy in the United States | Department of Energy [Internet]. [2020 May 31]. Available from: https://www.energy.gov/eere/solarpoweringamerica/solar-energy-united-states

[11] Koebrich S, Tian T, Chen E. 2017 Renewable Energy Data Book Including Data and Trends for Energy Storage and Electric Vehicles Acknowledgments.

[12] About Solar Energy | SEIA [Internet]. [2020 May 30]. Available from: https://www.seia.org/initiatives/about-solar-energy

[13] Photovoltaics and electricity - U.S. Energy Information Administration (EIA) [Internet]. [2020 Jun 8]. Available from: https://www.eia.gov/energyexplained/solar/photovoltaics-and-electricity.php

[14] Suskis P, Galkin I. Enhanced photovoltaic panel model for MATLAB-simulink environment considering solar cell junction capacitance. In: IECON Proceedings (Industrial Electronics Conference). 2013.

[15] Petrone G, Spagnuolo G, Teodorescu R, Veerachary M, Vitelli M. Reliability issues in photovoltaic power processing systems. IEEE Transactions on Industrial Electronics. 2008;

[16] Ayompe LM, Duffy A. Thermal performance analysis of a solar water heating system with heat pipe evacuated tube collector using data from a field trial. Solar Energy. 2013;

[17] Turchi CS, Ma Z, Neises TW, Wagner MJ. Thermodynamic study of advanced supercritical carbon dioxide power cycles for concentrating solar power systems. Journal of Solar Energy Engineering, Transactions of the ASME. 2013;

[18] Mehos M, Turchi C, Vidal J, Wagner M, Ma Z, Ho C, et al. Concentrating Solar Power Gen3 Demonstration Roadmap. Nrel/Tp-5500-67464. 2017;

[19] Castillo A. Is CSP an expensive or a viable investment? | New Energy Update [Internet]. 2015. Available from: https://analysis.newenergyupdate.com/csp-today/markets/csp-expensive-or-viable-investment

[20] dos MA, Voß A, Weinrebe G. Thermal and technical analyses of solar chimneys. Solar Energy. 2003 Dec 1;75(6):511–24.

[21] Maia CB, Silva FVM, Oliveira VLC, Kazmerski LL. An overview of the use of

solar chimneys for desalination. Vol. 183, Solar Energy. Elsevier Ltd; 2019. p. 83–95.

[22] Flat plate collectors vs evacuated tube collectors - Simple Solar [Internet]. [2020 Jun 30]. Available from: https://www.simplesolar.ca/flat-plate-collectors-vs-evacuated-tube-collectors.html

[23] Behnam P, Shafii MB. Examination of a solar desalination system equipped with an air bubble column humidifier, evacuated tube collectors and thermosyphon heat pipes. Desalination. 2016;

[24] Kalogirou SA. Nontracking solar collection technologies for solar heating and cooling systems. In: Advances in Solar Heating and Cooling. 2016.

[25] Balaras CA, Grossman G, Henning HM, Infante Ferreira CA, Podesser E, Wang L, et al. Solar air conditioning in Europe-an overview. Renewable and Sustainable Energy Reviews. 2007;11(2):299–314.

[26] Auyeung N, Kreider P. Solar Thermochemical Energy Storage | AIChE [Internet]. [2020 Jun 21]. Available from: https://www.aiche.org/resources/publications/cep/2017/july/solar-thermochemical-energy-storage

[27] Abhat A. LOW TEMPERATURE LATENT HEAT THERMAL ENERGY STORAGE: HEAT STORAGE MATERIALS. Vol. 10, Solar Ene, T¢~.

[28] Heat transfer enhancement of phase change materials for thermal energy storage applications_ A critical review | Elsevier Enhanced Reader [Internet]. [2020 May 31]. Available from:

https://reader.elsevier.com/reader/sd/pii/S1364032117301739?token=CF243D6D2DAB2C37652CF606507F2207AE2A389A251F0478828A93BA339A5562EC033835974086E76669220CC42D6865

[29] Al-Abidi AA, Bin Mat S, Sopian K, Sulaiman MY, Mohammed AT. CFD applications for latent heat thermal energy storage: A review. Renewable and Sustainable Energy Reviews. 2013.

[30] Castellani B, Morini E, Filipponi M, Nicolini A, Palombo M, Cotana F, et al. Clathrate hydrates for thermal energy storage in buildings: Overview of proper hydrate-forming compounds. Sustainability (Switzerland). 2014.

[31] Karaipekli A, Sari A, Kaygusuz K. Thermal characteristics of paraffin/expanded perlite composite for latent heat thermal energy storage. Energy Sources, Part A: Recovery, Utilization and Environmental Effects. 2009;31(10):814–23.

[32] Agyenim F, Eames P, Smyth M. A comparison of heat transfer enhancement in a medium temperature thermal energy storage heat exchanger using fins. Solar Energy. 2009;83(9):1509–20. Available from: http://dx.doi.org/10.1016/j.solener.2009.04.007

[33] Dmitruk A, Naplocha K, Grzęda J, Kaczmar JW. Aluminum inserts for enhancing heat transfer in PCM accumulator. Materials. 2020;13(2).

[34] Sivasamy P, Devaraju A, Harikrishnan S. Review on Heat Transfer Enhancement of Phase Change Materials (PCMs). In: Materials Today: Proceedings. Elsevier Ltd; 2018. p. 14423–31.

[35] Chen J, Yang D, Jiang J, Ma A, Song D. Research Progress of Phase Change Materials (PCMs) Embedded with Metal Foam (a Review). Procedia Materials Science. 2014;4:389–94. Available from: http://dx.doi.org/10.1016/j.mspro.2014.07.579

[36] Mettawee EBS, Assassa GMR. Thermal conductivity enhancement in a latent heat storage system. Solar Energy. 2007;81(7):839–45.

[37] Md Mahamudur Rahman, Han Hu, Hamidreza Shabgard, Philipp Boettcher, Ying Sun MM. Experimental Characterization of Inward Freezing and Melting of Additive-Enhanced Phase-Change Materials Within Millimeter-Scale Cylindrical Enclosures. ASME J Heat Transfer. 2016;(072301):13.

[38] Fukai J, Hamada Y, Morozumi Y, Miyatake O. Effect of carbon-fiber brushes on conductive heat transfer in phase change materials. International Journal of Heat and Mass Transfer. 2002;45(24):4781–92.

[39] Seeniraj R V., Lakshmi Narasimhan N. Performance enhancement of a solar dynamic LHTS module having both fins and multiple PCMs. Solar Energy. 2008;82(6):535–42.

[40] Shabgard H, Allen MJ, Sharifi N, Benn SP, Faghri A, Bergman TL. Heat pipe heat exchangers and heat sinks: Opportunities, challenges, applications, analysis, and state of the art. Vol. 89, International Journal of Heat and Mass Transfer. Elsevier Ltd; 2015. p. 138–58.

[41] Sharifi N, Bergman TL, Allen MJ, Faghri A. Melting and solidification

enhancement using a combined heat pipe, foil approach. International Journal of Heat and Mass Transfer. 2014;78:930–41. Available from: http://dx.doi.org/10.1016/j.ijheatmasstransfer.2014.07.054

[42] V Mittal, KS Kasana, NS Thakur. The study of solar absorption air-conditioning systems. Journal of Energy in Southern Africa @BULLET. 2005;16(4):59–66. Available from: http://www.erc.uct.ac.za/sites/default/files/image_tool/images/119/jesa/16-4jesa-mittal.pdf

[43] Ketfi O, Merzouk M, Merzouk NK, Metenani S El. Performance of a Single Effect Solar Absorption Cooling System (Libr-H2O). In: Energy Procedia. 2015.

[44] Marc O, Sinama F, Praene JP, Lucas F, Castaing-Lasvignottes J. Dynamic modeling and experimental validation elements of a 30 kW LiBr/H2O single effect absorption chiller for solar application. Applied Thermal Engineering. 2015;

[45] Philander SG, Koslowsky RK. Solar Energy Industries Association. In: Encyclopedia of Global Warming & Climate Change. 2012.

[46] Latent-Heat based Thermal Energy Storage technology for building scale applications - RE-COGNITION [Internet]. [2020 Jun 2]. Available from: https://re-cognition-project.eu/2020/03/12/latent-heat-based-thermal-energy-storage-technology-for-building-scale-applications/

[47] Bland A, Khzouz M, Statheros T, Gkanas EI. PCMs for residential building

applications: A short review focused on disadvantages and proposals for future development. Buildings. 2017;7(3).

[48] Kossecka E, J K. Thermal Balance of a One-Dimensional Sample of Pcm-Enhanced Thermal Insulation. (2):265–71. Available from: http://www.ippt.pan.pl/Repository/o104.pdf

[49] Hawes DW, Feldman D, Banu D. Latent heat storage in building materials. Energy and Buildings. 1993;20(1):77–86.

[50] Castellon C, Castell A, Medrano M, Martorell L. Experimental Study of PCM Inclusion in Different Building Envelopes. Journal of Solar Energy Engineering, Transactions of the ASME. 2009;(041006):6. Available from: https://asmedigitalcollection.asme.org/solarenergyengineering/article-abstract/131/4/041006/447661/Experimental-Study-of-PCM-Inclusion-in-Different?redirectedFrom=PDF

[51] Chaiyat N. Energy and economic analysis of a building air-conditioner with a phase change material (PCM). Energy Conversion and Management. 2015 Apr 1;94:150–8.

[52] Esen M. Thermal performance of a solar-aided latent heat store used for space heating by heat pump. Solar Energy. 2000 Jan 1;69(1):15–25.

[53] Du S, Wang RZ, Lin P, Xu ZZ, Pan QW, Xu SC. Experimental studies on an air-cooled two-stage NH3-H2O solar absorption air-conditioning prototype. Energy. 2012;45(1):581–7.

[54] Fabi V, Andersen RV, Corgnati S, Olesen BW. Occupants' window opening

behaviour: A literature review of factors influencing occupant behaviour and models. Building and Environment. 2012 Dec 1;58:188–98.

[55] Yu Z, Fung BCM, Haghighat F, Yoshino H, Morofsky E. A systematic procedure to study the influence of occupant behavior on building energy consumption. Energy and Buildings. 2011 Jun 1;43(6):1409–17.

[56] Mesalhy O, Lafdi K, Elgafy A, Bowman K. Numerical study for enhancing the thermal conductivity of phase change material (PCM) storage using high thermal conductivity porous matrix. Energy Conversion and Management. 2005 Apr 1;46(6):847–67.

[57] Cengel YA, Boles MA. Thermodynamics: an Engineering Approach 8th Edition. McGraw-Hill. 2015.

[58] Climate Zones | Department of Energy [Internet]. [2020 Jun 1]. Available from: https://www.energy.gov/eere/buildings/climate-zones

[59] Recent changes to ASHRAE and IECC climate zone map and building codes [Internet]. [2020 Jun 1]. Available from: https://www.pepperconstruction.com/blog/science-building-codes-and-climate-zones

[60] Baechler, Williamson, Gilbride, Cole, Hefty L. Building America climate zone map | Building America Solution Center [Internet]. [2020 Jun 29]. Available from: https://basc.pnnl.gov/images/building-america-climate-zone-map

[61] Index of /datasets/files/961/pub/EPLUS_TMY2_RESIDENTIAL_BASE

[Internet]. [2020 Jun 1]. Available from: https://openei.org/datasets/files/961/pub/EPLUS_TMY2_RESIDENTIAL_BASE/

[62] Payne W V, Domanski PA, Payne WV, Domanski PA. Purdue e-Pubs A Comparison Of An R22 And An R410A Air Conditioner Operating At High Ambient Temperatures A Comparison of an R22 and an R410A Air Conditioner Operating at High Ambient Temperatures [Internet]. [2020 Jun 1]. Available from: http://docs.lib.purdue.edu/iracc/532

[63] COPs, EERs, and SEERs – Power Knot SRA [Internet]. [2020 Jun 1]. Available from: https://powerknotsra.com/2011/03/01/cops-eers-and-seers/

[64] NSRDB: 1991- 2010 Update [Internet]. [2020 Jun 1]. Available from: https://rredc.nrel.gov/solar/old_data/nsrdb/1991-2010/

[65] (No Title) [Internet]. [2020 May 31]. Available from: https://www.nrel.gov/docs/fy11osti/52172.pdf

[66] States Department of Energy U. Combined Heat and Power Technology Fact Sheet Series ADVANCED MANUFACTURING OFFICE.

[67] Magnesium Nitrate Hexahydrate | AMERICAN ELEMENTS ® [Internet]. [2020 Jun 4]. Available from: https://www.americanelements.com/magnesium-nitrate-hexahydrate-13446-18-9

[68] Zalba B, Marín JM, Cabeza LF, Mehling H. Review on thermal energy

storage with phase change: Materials, heat transfer analysis and applications. Vol. 23, Applied Thermal Engineering. Pergamon; 2003. p. 251–83.

[69] Bhattacharya A, Calmidi V V., Mahajan RL. Thermophysical properties of high porosity metal foams. International Journal of Heat and Mass Transfer. 2002 Jan 8;45(5):1017–31.

[70] Quarter (Q1, Q2, Q3, Q4) Definition [Internet]. [2020 Jun 2]. Available from: https://www.investopedia.com/terms/q/quarter.asp

[71] EIA - Electricity Data [Internet]. [2020 Jun 2]. Available from: https://www.eia.gov/electricity/monthly/epm_table_grapher.php?t=epmt_5_6_a

[72] Calculate Energy Usage with EMS' Energy Tools [Internet]. [2020 Jun 2]. Available from: http://www.emsenergy.com/energy-tools/

[73] Alva G, Lin Y, Fang G. An overview of thermal energy storage systems. Vol. 144, Energy. Elsevier Ltd; 2018. p. 341–78.

APPENDIX

Tables

T1. Solar utilization ratio

City	TES (kWh)	Collector area (m^2)	Energy savings per unit PCM mass (kWh/kg)	Energy savings per unit area (kWh/m^2)	Solar utilization ratio
Miami, FL	07.46	08.04	39.44	828.54	0.80
	14.91	16.07	31.02	651.64	0.63
	22.37	24.11	25.74	540.71	0.52
Duluth, MN	26.94	078.46	35.57	408.62	0.35
	53.88	156.92	26.28	250.50	0.26
	80.82	235.38	21.48	170.10	0.21
Oklahoma City, OK	10.77	19.59	38.47	479.04	0.47
	21.54	39.17	28.44	354.11	0.35
	32.31	58.76	23.03	286.78	0.28
Albuquerque, NM	09.81	11.36	45.73	894.53	0.73
	19.62	22.71	28.81	563.54	0.46
	29.43	34.07	24.79	484.88	0.39
Los Angeles, CA	03.81	05.52	43.67	681.49	0.64
	07.61	11.04	34.50	538.47	0.51
	11.42	16.56	27.86	434.80	0.41
Reno, NV	18.195	28.20	33.69	492.17	0.43
	36.39	56.40	25.73	375.93	0.34
	54.59	84.60	21.02	307.13	0.28
Portland, OR	11.37	43.14	37.76	225.23	0.30
	22.73	86.28	27.66	165.01	0.22
	34.10	129.42	22.86	136.34	0.17

Complementary Figures (CF)

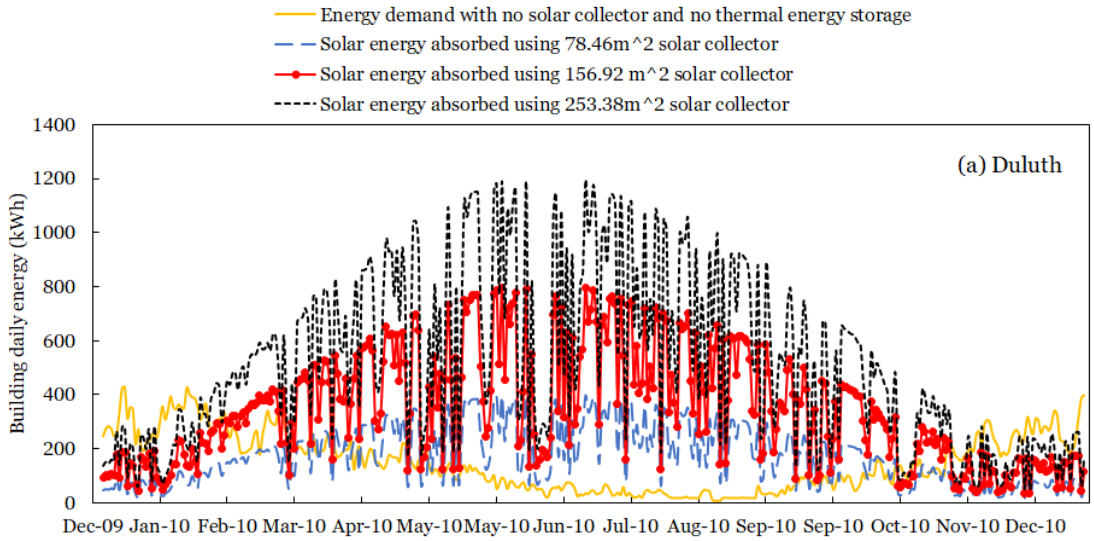

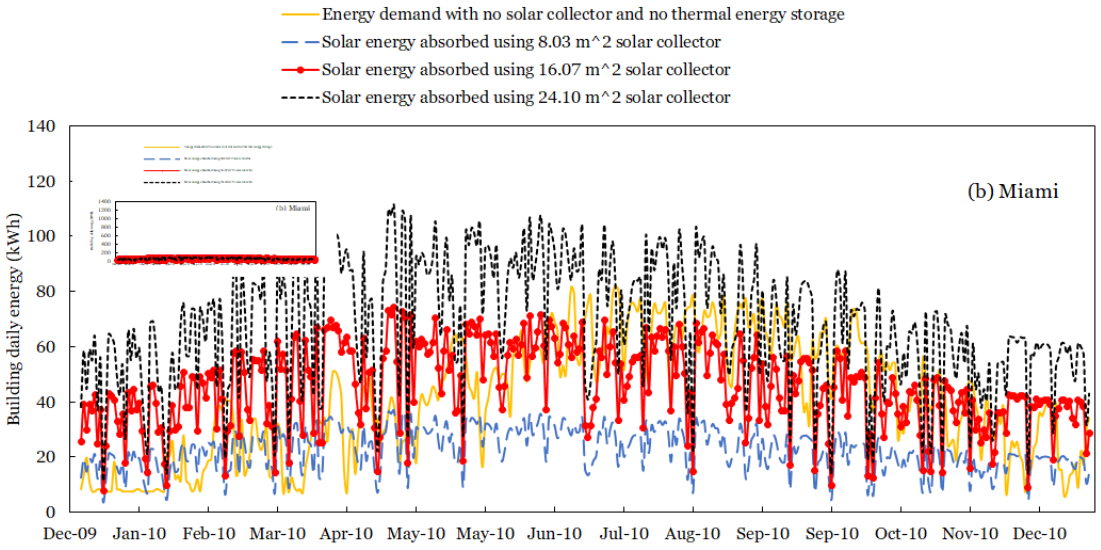

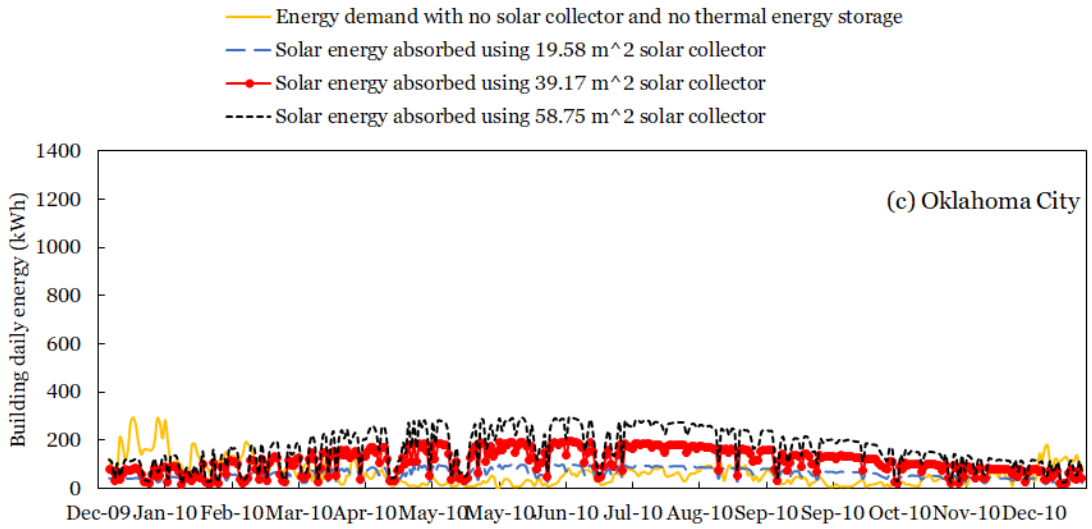
Energy demand with no solar collector and no thermal energy storage
Solar energy absorbed using 19.58 m^2 solar collector
Solar energy absorbed using 39.17 m^2 solar collector
Solar energy absorbed using 58.75 m^2 solar collector
(c) Oklahoma City
Building daily energy (kWh)
1400
1200
1000
800
600
400
200
0
Dec-09 Jan-10 Feb-10 Mar-10 Apr-10 May-10 May-10 Jun-10 Jul-10 Aug-10 Sep-10 Sep-10 Oct-10 Nov-10 Dec-10

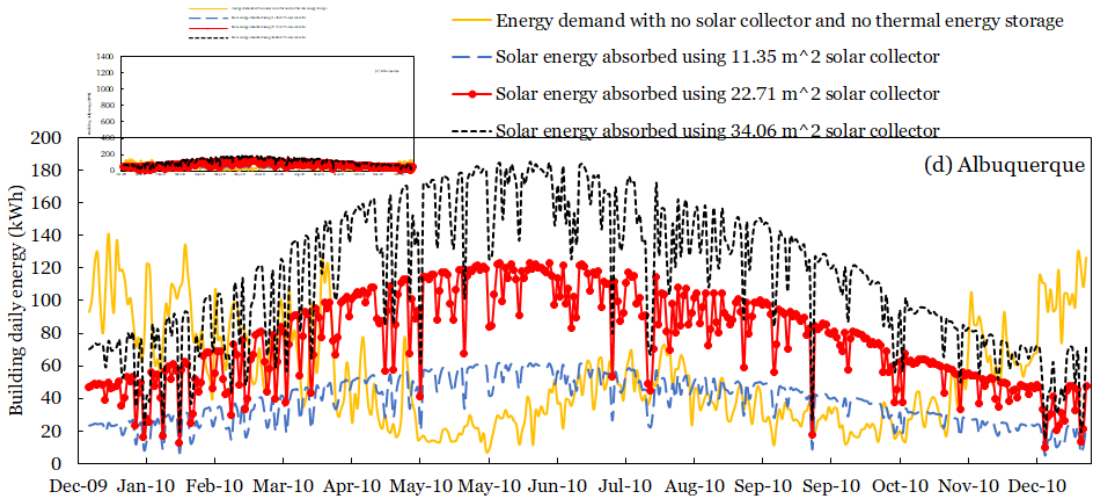
Energy demand with no solar collector and no thermal energy storage
Solar energy absorbed using 11.35 m^2 solar collector
Solar energy absorbed using 22.71 m^2 solar collector
Solar energy absorbed using 34.06 m^2 solar collector
(d) Albuquerque
Building daily energy (kWh)
200
180
160
140
120
100
80
60
40
20
0
Dec-09 Jan-10 Feb-10 Mar-10 Apr-10 May-10 May-10 Jun-10 Jul-10 Aug-10 Sep-10 Sep-10 Oct-10 Nov-10 Dec-10

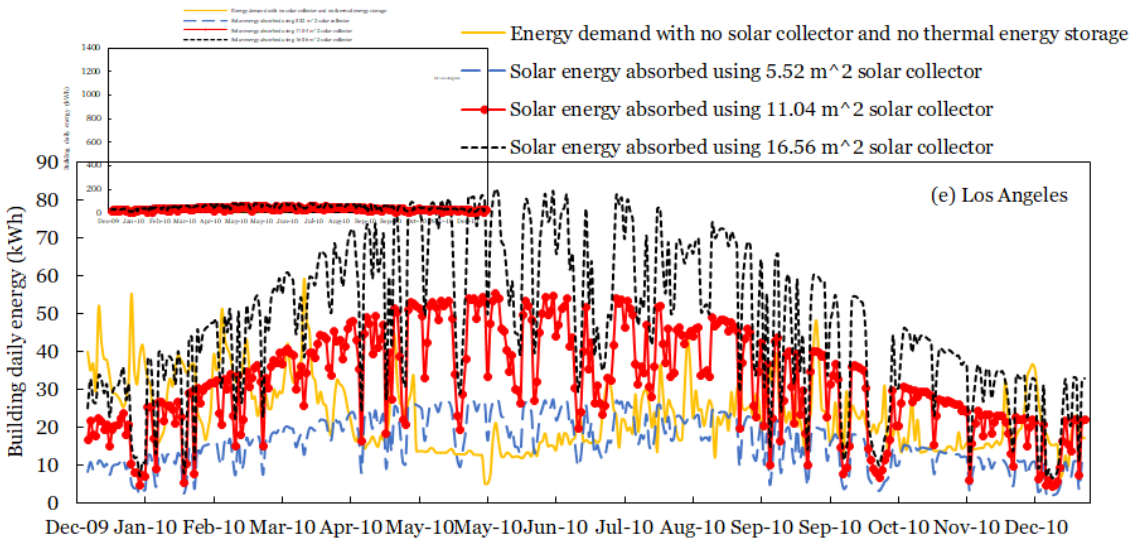
Energy demand with no solar collector and no thermal energy storage
Solar energy absorbed using 5.52 m^2 solar collector
Solar energy absorbed using 11.04 m^2 solar collector
Solar energy absorbed using 16.56 m^2 solar collector
(e) Los Angeles
Building daily energy (kWh)
0
10
20
30
40
50
60
70
80
90
Dec-09 Jan-10 Feb-10 Mar-10 Apr-10 May-10 May-10 Jun-10 Jul-10 Aug-10 Sep-10 Sep-10 Oct-10 Nov-10 Dec-10

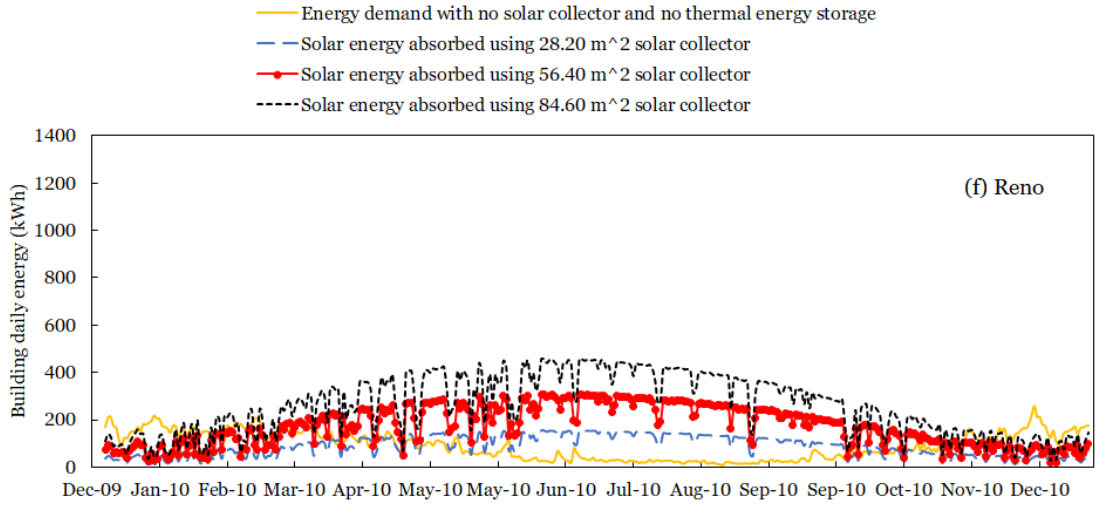
Energy demand with no solar collector and no thermal energy storage
Solar energy absorbed using 28.20 m^2 solar collector
Solar energy absorbed using 56.40 m^2 solar collector
Solar energy absorbed using 84.60 m^2 solar collector
(f) Reno
Building daily energy (kWh)
0
200
400
600
800
1000
1200
1400
Dec-09 Jan-10 Feb-10 Mar-10 Apr-10 May-10 May-10 Jun-10 Jul-10 Aug-10 Sep-10 Sep-10 Oct-10 Nov-10 Dec-10

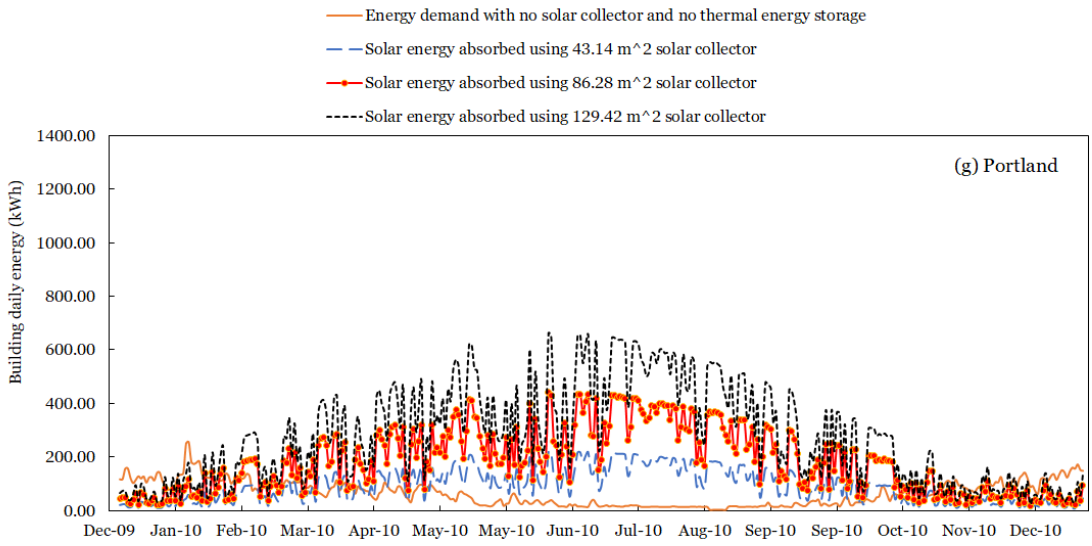

CF 1. (a) – (g) Annual total building energy and the absorbed solar energy

MATLAB code

```
%******************************** Main ************************************
%**************************************************************************
close all
clear all
clc
tic
global ri ro r twh kw Nelm Ns Nl LST NHP
global tallmelt STATE Sdotin Sdotout Qdotout Qdotin Exin Exout dSdt
global Lh Lw La Lb aw
global Tm hsl kL kS cL aL aS rhoL rhoS Esen Load_Solar
global Ti dlqd dsld A Mass TPCMavg dms qin Qaux

global totalqsolar totalload
%**************************************
% Effective PCM Properties
%**************************************
eps = 0.98;
Tm = 89 + 273.15;
rhoPCML = 1550;
kPCML = 0.5;
cPCML = 554;
hslPCM = 162.8e3;
rhor = 1;
kr = 1;
cr = 1;
rhoPCMS = rhoPCML*rhor;
kPCMS = kPCML*kr;
cPCMS = cPCML*cr;

rhometal = 2700;
kmetal = 205;
cmetal = 900;

kL    =    (kPCML+pi*(sqrt((1-eps)/3/pi)-(1-eps)/3/pi)*(kmetal-kPCML))*(kPCML+(1-
eps)/3*(kmetal-kPCML))/...
    (kPCML+(4/3*sqrt((1-eps)/3/pi)*(1-eps)+pi*sqrt((1-eps)/3/pi)-(1-
eps))*(kmetal-kPCML));
cL = eps*cPCML+(1-eps)*cmetal;
rhoL = eps*rhoPCML+(1-eps)*rhometal;

kS    =    (kPCMS+pi*(sqrt((1-eps)/3/pi)-(1-eps)/3/pi)*(kmetal-kPCMS))*(kPCMS+(1-
eps)/3*(kmetal-kPCMS))/...
    (kPCMS+(4/3*sqrt((1-eps)/3/pi)*(1-eps)+pi*sqrt((1-eps)/3/pi)-(1-
eps))*(kmetal-kPCMS));
cS = eps*cPCMS+(1-eps)*cmetal;
rhoS = eps*rhoPCMS+(1-eps)*rhometal;

hsl = eps*hslPCM;
aL = kL/(rhoL*cL);
aS = kS/(rhoS*cS);

%**************************************
% Heat Pipe Specifications
```

```
%**************************************
ri = 0.015;
Dwho = 2*ri;
twh = 0.002;
Dwhi = Dwho - 2*twh;
kw = 16;
aw = kw/(7900*400);
Lh = 1.;
Lw = 0.1;
La = 0.2;
Lb = 0.2;
Rwh = log(Dwho/Dwhi)/(2*pi*kw*Lh);
%**************************************
% BUNDLE ARRANGEMENT
%**************************************
TES=;
MTES=TES*3600/159;
MPCM = MTES.*hslPCM/hsl;
L = 0.125;%(MPCM/(NHP*Lh*rhoL)+2*pi*ri^2)^0.5          %unit cell length
ro = L/sqrt(2*pi);
%MPCM = NHP*(L^2-2*pi*ri^2)*Lh*rhoL;
NHP=MPCM/((L^2-2*pi*ri^2)*Lh*rhoL);
MPCM = NHP*(L^2-2*pi*ri^2)*Lh*rhoL;
% MPCM = 670.6305;
%**************************************
% TN Model Specifications
%**************************************
NN = 8;
Ns = NN;
Nl = NN;
Nelm = Ns + Nl + 6;
LST = 1 + Nl + Ns;
%**************************************
% INITIAL CONDITIONS
%**************************************
T0 = 300;
yin = zeros(Nelm,1)+Tm-0.1;
yin(1:Nl+1,1) = Tm+0.1;
 f0 = 0.5;
 Mass = f0*(2*(ro^2-ri^2));
if (f0<=0.5)
    yin(end) = sqrt(Mass+ri^2)-ri;
else
    yin(end) = -sqrt((ro^2-ri^2+ro^2)-Mass) + 2*ro - ri;
end
%yin(1) = Tm + 0.4*10;
%yin(Nl+Ns+2) = Tm-10;
TPCMag(1,1) = Tm;
del = L/200;
f(1) = f0;
tallmelt = 0;
STATE = 0;
j = 0;
Ex(1,1:5) = 0;
totalqsol =0;
totaload = 0;

%**************************************
```

```
% PCM MASS
%**************************************

loadC=[];
loadH=[];
loadw=[];
qsolar=[];
Asolar=;
i = 1;
BB = 0;
duration = 8760;

%for t = 1:duration*3600
%
% tday = floor(t/3600)+1;
% % if (tday>24)
% %     tday = tday-24;
% % end
% if mod(tday,24)==1 %%% to start a new day
%     tday=1;
% end
%
% tday0 = tday-1;
% if tday0==0
%     tday0 = 24;
% end
% tfrac = (t/3600)-floor(t/3600);
% qsolart = qsolar(tday0)+tfrac*(qsolar(tday)-qsolar(tday0));
% loadwt = (loadw(tday0)+tfrac*(loadw(tday)-loadw(tday0)))*1000;
% loadHt = (loadH(tday0)+tfrac*(loadH(tday)-loadH(tday0)))*1000;
% qin = qsolart*Asolar*0.6;         % collector area = 10 m2; efficiency 60%
% BB = BB + (qin-(loadwt+loadHt))*1;
% if abs(loadwt+loadHt-qin)<.1
%     B = BB/hsl;
%     BB = 0;
%     teqal(i) = t;
%     i = i+1;
% end
% end

% %**************************************
% MAIN
%**************************************

Dt = 900;
for i = 0:Dt:duration*3600
    j = j+1;
    t1 = i;
    t2 = t1+Dt;
    Mass_old = Mass;
    if (t1>11.8*3600)
        aaa= 0;
    end
    if yin(end)>=del && yin(end)<=(2*(ro-ri)-del)
        [T,Y] = ode45(@January,(t1:Dt/2:t2),yin);
        if (j==1)
            Mass_old = Mass;
```

```
        end
    elseif yin(end)<=(2*(ro-ri)-del)
        [T,Y] = ode45(@Jan_subcool,(t1:Dt/2:t2),yin);
        if Y(end,1)>Tm
            STATE = 0;
            Y(end,end) = 1.05*del;
        end
    elseif yin(end)>=del
        [T,Y] = ode45(@Jan_superheat,(t1:Dt/2:t2),yin);
        if Y(end,LST+1)<Tm
            STATE = 0;
            Y(end,end) = 2*(ro-ri)-1.05*del;
        end
    end

    solution(j*2-1:j*2+1,1) = T;
    solution(j*2-1:j*2+1,2:Nelm+1) = Y;
    yin = Y(end,:);

    totalqsol =totalqsolar*Dt/1000/3600+totalqsol;
    totaload = totalload*Dt/1000/3600+totaload;

    if abs(totalqsolar/1000-totalload/1000)<.01
        if(T(end)/3600<10)
            eqault1=T(end);
            qPCM1 = totaload-totalqsol;
        else
            eqault2=T(end);
            %qPCM2 = totalqsol-(totaload-qPCM1);
        end
    end


%****************************************
% ENTROPY
%****************************************
    dSsys = 0;
    Qdotsys = 0;

    if (yin(end)<=ro-ri)
        M = (yin(end)+ri)^2-ri^2;
    else
        M = ro^2-ri^2 + ro^2 - (2*ro-(yin(end)+ri))^2;
    end
    f(j+1) = M/(2*(ro^2-ri^2));
%     for k = 2:LST
%         if k<=Nl+1
%             Tavg = Tavg + Y(end,k)*2*dlqd;
%         else
%             Tavg = Tavg + Y(end, k)*2*dsld;
%     end
    for k = 1:LST+4
        if (k<2) || (k>LST)
            deltaT = Y(end,k)-Y(1,k);
            Tavg = (Y(end,k)+Y(1,k))/2;
            heatcapac = 400;
            dSsys = dSsys + pi*Lh*heatcapac*Mass(k)*log(Y(end,k)/Y(1,k));
```

```
            Qdotsys = Qdotsys + pi*Lh*heatcapac*Mass(k)*(Y(end,k)-Y(1,k))/Dt;
        end
    end
    Qdot_latent = (f(j+1)-f(j))*(2*(ro^2-ri^2))*pi*Lh*rhoL*hsl/Dt;
    TPCMag(j,1)    =    -(Qdotin-Qdotout-Qdotsys-Qdot_latent)*Dt/(2*pi*Lh*(ro^2-
ri^2)*rhoL*cL)+TPCMavg;

        dSsys = dSsys + 2*pi*Lh*(ro^2-ri^2)*rhoL*cL*log(TPCMavg/TPCMag(end));
        Qdotsys    =    Qdotsys    +    (2*pi*Lh*(ro^2-ri^2)*rhoL*cL*(TPCMavg-
TPCMag(end)))/Dt;
        Exsys = (Qdot_latent+Qdotsys)-300*(dSsys/Dt + Qdot_latent/Tm);

    Sdot(j,1) = t2;
    Sdot(j,2) = -Sdotin;
    Sdot(j,3) = Sdotout;
    Sdot(j,4) = dSsys/Dt;
    Sdot(j,5) = Qdot_latent/Tm;
    Sdot(j,6) = max(0,sum(Sdot(j,2:5)));
    Sdot(j,7) = (dSdt(Nelm))*pi*Lh;
    Sdot(j,8) = sum(dSdt(1:Nelm-1))*pi*Lh;
    Sdot(j,9) = Sdot(j,4)+Sdot(j,5);
    dSdtt(j,:) = dSdt;

    Ex(j+1,1) = t2/3600;
    Ex(j+1,2) = Ex(j,2) + Exin;
    Ex(j+1,3) = Ex(j,3) + Exout;
    Ex(j+1,4) = Ex(j,4) + Exsys;
    Ex(j+1,5) = Ex(j,5) + Exin-Exout-Exsys;
    Ex(j+1,6) = 1-(Exin-Exout-Exsys)/Exin;
    Ex(j+1,7) = Exin;
    Ex(j+1,8) = Exout;
    Ex(j+1,9) = dms;
    Ex(j+1,10) = totalqsolar;
    Ex(j+1,11) = totalload;
    Ex(j+1,12) = Qaux;
    LS(j,:) = Load_Solar/1000;


    if Sdot(j,6)<0
        dsaf = 1;
    end

%*********************************************
    if yin(end)>=del && yin(end)<=(2*(ro-ri)-del)
        if dlqd<2*del && Nl>1
            Nl = Nl/2;
        end
        if dlqd>5*del && Nl<NN
            Nl = Nl*2;
        end
        if dsld<2*del && Ns>1
            Ns = Ns/2;
        end
        if dsld>5*del && Ns<NN
            Ns = Ns*2;
        end
    end
```

```
end
%**************************************
% MAIN END
%**************************************

toc

%%%*************************** Subcool sub-routine *****************
%*****************************************************************
function [dy]= subcooled(t,y)

global ri ro r twh kw Nelm Ns Nl LST NHP
global tallmelt STATE Sdotin Sdotout Qdotout Qdotin Exin Exout dSdt
global Lh Lw La Lb aw
global Tm hsl kL kS cL aL aS rhoL rhoS Esen Load_Solar
global Ti dlqd dsld A Mass TPCMavg
global totalqsolar totalload Qaux dms

%Tm = 1000;
hw = 2000;
ha = 500;
hb = 0.0;

mdotw = 0.0;
mdota = 0.0;
cpw = 4200;
cpa = 1000;
Tinw = 20;
Tina = 20;
TLiBr = 80;

%************************************
loadC=[];
loadH=[];
loadw=[];
qsolar=[];
Asolar=;

tday = floor(t/3600)+1;
if mod(tday,8760)==1
     tday=8760;
end
tday0 = tday-1;
if tday0==0
    tday0 = 8760;
end
tfrac = (t/3600)-floor(t/3600);
qsolart = qsolar(tday0)+tfrac*(qsolar(tday)-qsolar(tday0));
loadwt = (loadw(tday0)+tfrac*(loadw(tday)-loadw(tday0)))*1000;
loadHt = (loadH(tday0)+tfrac*(loadH(tday)-loadH(tday0)))*1000;
loadCt = (loadC(tday0)+tfrac*(loadC(tday)-loadC(tday0)))*1000;
qin = qsolart*Asolar*0.6;         % collector area = 10 m2; efficiency 60%
qin1 = qin/NHP;


Tsath = (y(1) + qin1*(twh/2)/(kw*pi*(2*ri-twh)*Lh));
```

```
if Tsath>=383.15
    qin=0;
    qin1 = qin/NHP;
    Tsath=y(1);
end
Qaux=0;

%*****************************************************************

dy = zeros(Nelm,1);
Aw = A(LST+1)*Lw/Lh;
Aa = A(LST+1)*La/Lh;
Ab = A(LST+1)*Lb/Lh;
Ti(1) = Tsath;
dsld1 = A(LST-Ns+1)-ri;
Ti(LST-Ns+1) = (y(LST-Ns+1)*kS*A(LST-Ns+1)/dsld1+y(1)*kw*A(1)/(twh/2))/...
    (kw*A(1)/(twh/2)+kS*A(LST-Ns+1)/dsld1);

for i = LST-Ns+1:LST
    if i == LST
        Ti(i+1)                                                          =
(y(LST)*kS*A(LST)/dsld+y(LST+1)*kw*A(LST+1)/(twh/2))/(kw*A(LST+1)/(twh/2)+kS*A(
LST)/dsld);
    else
        Ti(i+1) = (y(i)*A(i)+y(i+1)*A(i+1)) / (A(i)+A(i+1));
    end
    dy(i) = (Ti(i) - 2*y(i) + Ti(i+1)) * aS/(2*dsld^2);
end
dy(2:LST-Ns) = 0;
Tsatc                                                                    =
(y(LST+1)*A(LST+1)+y(LST+2)*Aw+y(LST+3)*Aa+y(LST+4)*Ab)/(A(LST+1)+Aw+Aa+Ab);

loadw1 = loadwt/NHP;
loadH1 = loadHt/NHP;
loadC1 = loadCt/NHP;
totalqsolar = qsolart*Asolar*0.6;
totalload = loadwt+loadHt+loadCt;
if Tsatc<=300
    Qaux=totalload;
    loadw1=0;
    loadH1=0;
    loadC1=0;
 end

%*****************************************************************
dy(1) = (Tsath - 2*y(1) + Ti(LST-Ns+1)) * aw/(2*(twh/2)^2);
dy(LST-Ns+1) = (Ti(LST-Ns+1) - y(LST-Ns+1))/dsld1 - (y(LST-Ns+1) - Ti(LST-
Ns+2))/dsld;
dy(LST-Ns+1) = aS*dy(LST-Ns+1)/(dsld1+dsld);
dy(LST+1) = (Ti(LST+1) - 2*y(LST+1) + Tsatc) * aw/(2*(twh/2)^2);

%*******************************
Tsw = y(LST+2)-loadw1*(twh/2)/(kw*Aw*2*pi*Lh);
Tsb = y(LST+4)-loadH1*(twh/2)/(kw*Ab*2*pi*Lh);
Tsa = y(LST+3)-loadC1*(twh/2)/(kw*Aa*2*pi*Lh);
%*******************************
Tsw = real(Tsw);
```

```
Tsw = min(y(LST+2),Tsw);
Tsa = min(y(LST+3),Tsa);
%Tsb = (y(LST+4)*kw/(twh/2) + TLiBr*hb)/(kw/(twh/2) + hb);
Tsb = min(y(LST+4),Tsb);

dy(LST+2) = (Tsw - 2*y(LST+2) + Tsatc) * aw/(2*(twh/2)^2);
dy(LST+3) = (Tsa - 2*y(LST+3) + Tsatc) * aw/(2*(twh/2)^2);
dy(LST+4) = (Tsb - 2*y(LST+4) + Tsatc) * aw/(2*(twh/2)^2);

if (t>5 && mod(t,300)<1.0)
    if (y(end)<=ro-ri)
        M = (y(end)+ri)^2-ri^2;
    else
        M = ro^2-ri^2 + ro^2 - (2*ro-(y(end)+ri))^2;
    end
    f = M/(2*(ro^2-ri^2));
    yo=1;
    [t/3600 y(1) y(LST+1) y(end)*1000 f qin/1000-(loadHt+loadwt+loadCt)/1000 Nl
Ns TPCMavg]
end
%TPCM = [Ti(LST-Ns+1); y(LST-Ns+1:LST); Ti(LST+1)];
dSdt = zeros(Nelm,1);
TPCMavg = 0;
MassPCM = 0;
Esen = 0;
for i = LST-Ns+1:LST
    Mass(i) = 2*A(i)*2*dsld*rhoS;
    if i==LST-Ns+1
        Mass(LST-Ns+1) = ((A(LST-Ns+1)+dsld)^2-ri^2)*rhoS;
    end
    TPCMavg = TPCMavg + Mass(i)*y(i);
    MassPCM = MassPCM + Mass(i);
    Esen = Esen + Mass(i)*cL*(y(i)-Tm);
    dSdt(i) = Mass(i)*cL*dy(i)/y(i);
end
TPCMavg = TPCMavg/MassPCM;
Mass(1) = 2*A(1)*twh*7900;
Mass(LST+1) = 2*A(LST+1)*twh*7900;
Mass(LST+2) = 2*Aw*twh*7900;
Mass(LST+3) = 2*Aa*twh*7900;
Mass(LST+4) = 2*Ab*twh*7900;
dSdt(1) = Mass(1)*400*dy(1)/y(1);
dSdt(LST+1) = Mass(LST+1)*400*dy(LST+1)/y(LST+1);
dSdt(LST+2) = Mass(LST+2)*400*dy(LST+2)/y(LST+2);
dSdt(LST+3) = Mass(LST+3)*400*dy(LST+3)/y(LST+3);
dSdt(LST+4) = Mass(LST+4)*400*dy(LST+4)/y(LST+4);
Esen = Esen + Mass(1)*400*(y(1)-Tm);
Esen = Esen + Mass(LST+1)*400*(y(LST+1)-Tm);
Esen = Esen + Mass(LST+2)*400*(y(LST+2)-Tm);
Esen = Esen + Mass(LST+3)*400*(y(LST+3)-Tm);
Esen = Esen + Mass(LST+4)*400*(y(LST+4)-Tm);

Sdotin = qin1/(Tsath);
Sdotout = loadw1/(Tsw) + loadH1/(Tsa) + loadC1/(Tsb);
Qdotout = loadw1 + loadH1 + loadC1;
Qdotin = qin1;
Exin = qin1*(1-300/Tsath);
Exout = loadw1*(1-300/Tsw) + loadH1*(1-300/Tsa) + loadC1*(1-300/Tsb);
```

```
Load_Solar = [NHP*(loadw1+loadH1+loadC1) NHP*qin1];
dms=max(0,totalload-totalqsolar);

%%%%*************************** Heattest sub-routine *************
%%%%*************************************************************

function [dy]= heattest(t,y)

global ri ro r twh kw Nelm Ns Nl LST NHP
global tallmelt STATE Sdotin Sdotout Qdotout Qdotin Exin Exout dSdt
global Lh Lw La Lb aw
global Tm hsl kL kS cL aL aS rhoL rhoS Esen Load_Solar
global Ti dlqd dsld A Mass TPCMavg
global totalqsolar totalload Qaux dms

hw = 2000;
ha = 500;
hb = 0.0;

mdotw = 0.0;
mdota = 0.0;
cpw = 4200;
cpa = 1000;
Tinw = 20;
Tina = 20;
TLiBr = 80;

%y(1) = max(y(1),Tm+1.e-3);
%***********************************

loadC=[];
loadH=[];
loadw=[];
qsolar=[];
Asolar=;



tday = floor(t/3600)+1;

if mod(tday,8760)==1
     tday=8760;
end
tday0 = tday-1;
if tday0==0
    tday0 = 8760;
end
tfrac = (t/3600)-floor(t/3600);
qsolart = qsolar(tday0)+tfrac*(qsolar(tday)-qsolar(tday0));
loadwt = (loadw(tday0)+tfrac*(loadw(tday)-loadw(tday0)))*1000;
loadHt = (loadH(tday0)+tfrac*(loadH(tday)-loadH(tday0)))*1000;
loadCt = (loadC(tday0)+tfrac*(loadC(tday)-loadC(tday0)))*1000;
qin = qsolart*Asolar*0.6;         % collector area = 10 m2; efficiency 60%
qin1 = qin/NHP;
Tsath = (y(1) + qin1*(twh/2)/(kw*pi*(2*ri-twh)*Lh));
if Tsath>=383.15
```

```
    qin=0;
    qin1 = qin/NHP;
    Tsath=y(1);
end
Qaux=0;
%*****************************************************************

Ste = cL*(Tsath-Tm)/hsl;

dy = zeros(Nelm,1);
s = y(Nelm);
%melting = 0;
dlqd = max(1.e-5,y(Nelm)/Nl/2);
dsld = (2*ro-(2*ri+max(0,y(Nelm))))/Ns/2;
if (abs(dsld)>100)
    dlqd = 1.e-4;
    dsld = (ro-(ri+dlqd))/Ns/2;
end

A = zeros(LST+1,1);
A(1) = ri-(twh/2);
A(2) = ri+dlqd;
for i = 3:Nl+1
    A(i) = A(i-1) + 2*dlqd;
end
A(LST-Ns+1) = ri+(dlqd*2*Nl)+dsld;
for i = LST-Ns+1:LST
    A(i) = (ri+(dlqd*2*Nl)+dsld) + (i-(LST-Ns+1))*2*dsld;
end
A(LST+1) = ri - twh/2;
Aw = A(LST+1)*Lw/Lh;
Aa = A(LST+1)*La/Lh;
Ab = A(LST+1)*Lb/Lh;
for i = 3:LST
    if (A(i)>0)
        delta = dlqd;
        if A(i)>(y(end)+ri)
            delta = dsld;
        end
        if (A(i)-delta>ro)
            A(i) = 2*ro - A(i);
        end
        if (A(i)+delta>ro && A(i)-delta<ro)
            A(i) = ro - delta;
        end
    end
end
Ti(1) = Tsath;
Ti(LST-Ns+1) = Tm;
for i = LST-Ns+1:LST
    if i == LST
        Ti(i+1)                                                                    =
(y(LST)*kS*A(LST)/dsld+y(LST+1)*kw*A(LST+1)/(twh/2))/(kw*A(LST+1)/(twh/2)+kS*A(
LST)/dsld);
    else
        Ti(i+1) = (y(i)*A(i)+y(i+1)*A(i+1)) / (A(i)+A(i+1));
    end
        dy(i) = (Ti(i) - 2*y(i) + Ti(i+1)) * aS/(2*dsld^2);
```

```
end
Tsatc
=(y(LST+1)*A(LST+1)+y(LST+2)*Aw+y(LST+3)*Aa+y(LST+4)*Ab)/(A(LST+1)+Aw+Aa+Ab);
loadw1 = loadwt/NHP;
loadH1 = loadHt/NHP;
loadC1 = loadCt/NHP;

totalqsolar = qsolart*Asolar*0.6;
totalload = loadwt+loadHt+loadCt;

if Tsatc<=300
    Qaux=totalload;
    loadw1=0;
    loadH1=0;
    loadC1=0;
end

%*****************************************************************

dy(LST+1) = (Ti(LST+1) - 2*y(LST+1) + Tsatc) * aw/(2*(twh/2)^2);
Tsw = y(LST+2)-loadw1*(twh/2)/(kw*Aw*2*pi*Lh);
Tsb = y(LST+4)-loadH1*(twh/2)/(kw*Ab*2*pi*Lh);
Tsa = y(LST+3)-loadC1*(twh/2)/(kw*Aa*2*pi*Lh);
%*******************************
Tsw = real(Tsw);
Tsw = min(y(LST+2),Tsw);
Tsa = min(y(LST+3),Tsa);
%Tsb = (y(LST+4)*kw/(twh/2) + TLiBr*hb)/(kw/(twh/2) + hb);
Tsb = min(y(LST+4),Tsb);
Tow = loadwt/(mdotw*cpw) + Tinw;
Toa = Tina + 1.e-3;
for i = 1:0
    qw = (mdotw*cpw)*(Tow-Tinw);
    Tsw = y(LST+2) - qw/(pi*2*ro*Lw)*(twh/2)/kw;
    Tsw = max(Tsw,Tow+1.e-5);
    DTlm = (Tow-Tinw)/log((Tsw-Tinw)/(Tsw-Tow));
    qw = hw * DTlm * (pi*2*ro*Lw);
    Tow  = qw/(mdotw*cpw) + Tinw;
    qa = (mdota*cpa)*(Toa-Tina);
    Tsa = y(LST+3) - qa/(pi*2*ro*La)*(twh/2)/kw;
    Tsa = max(Tsa,Toa+1.e-5);
    DTlma = (Toa-Tina)/log((Tsa-Tina)/(Tsa-Toa));
    qa = ha * DTlma * (pi*2*ro*La)
    Toa  = qa/(mdota*cpa) + Tina;
end
dy(LST+2) = (Tsw - 2*y(LST+2) + Tsatc) * aw/(2*(twh/2)^2);
dy(LST+3) = (Tsa - 2*y(LST+3) + Tsatc) * aw/(2*(twh/2)^2);
dy(LST+4) = (Tsb - 2*y(LST+4) + Tsatc) * aw/(2*(twh/2)^2);

if (t>5 && mod(t,100)<1.0)
    if (y(end)<=ro-ri)
        M = (y(end)+ri)^2-ri^2;
    else
        M = ro^2-ri^2 + ro^2 - (2*ro-(y(end)+ri))^2;
    end
    f = M/(2*(ro^2-ri^2));
    yo=1;
```

```
    [t/3600 y(1) y(LST+1) y(end)*1000 f qin/1000-(loadHt+loadwt+loadCt)/1000 Nl
Ns TPCMavg]
end
TPCM = [Ti(2); y(2:Nl+1); Tm; y(LST-Ns+1:LST); Ti(LST+1)];
Ti(1:LST+1) = 0;
Ti(2) = (y(1)*kw*A(1)/(twh/2)+y(2)*kL*A(2)/dlqd)/...
    (kw*A(1)/(twh/2)+kL*A(2)/dlqd);
Ti(Nl+2) = Tm;
for i = 2:Nl
    Ti(i+1) = (y(i)*A(i)+y(i+1)*A(i+1)) /(A(i)+A(i+1));
    dy(i) = (Ti(i) - 2*y(i) + Ti(i+1)) * aL/(2*dlqd^2);
end
dy(1) = (Tsath - 2*y(1) + Ti(2)) * aw/(2*(twh/2)^2);
dy(Nl+1) = (Ti(Nl+1) - 2*y(Nl+1) + Ti(Nl+2)) * aL/(2*dlqd^2);

qout = kS*2*A(LST-Ns+1)*(Tm-y(LST-Ns+1))/dsld;
qout = max(0,qout);
qin = kL*2*A(Nl+1)*(y(Nl+1)-Tm)/dlqd;
qin = max(0,qin);
dV = max(-1e8,(qin-qout)/(rhoS*hsl));
if (y(Nelm)<=ro-ri)
    dy(Nelm) = dV/2/(y(Nelm)+ri);
else
%    M = ro^2-ri^2 + ro^2 - (2*ro-(y(end)+ri))^2;
    dy(Nelm) = dV/2/(2*ro-(y(Nelm)+ri));
end
s = y(Nelm);

r = zeros(Nl+Ns+3,1);
r = [A(2)-dlqd; A(2:Nl+1); y(end)+ri; A(LST-Ns+1:LST); A(LST)-dsld];
TPCM(1) = Ti(2);

TPCMavg = 0;
MassPCM = 0;
Esen = 0;
dSdt = zeros(Nelm,1);
for i = 2:Nl+1
    Mass(i) = 2*A(i)*2*dlqd*rhoL;
    TPCMavg = TPCMavg + Mass(i)*y(i);
    MassPCM = MassPCM + Mass(i);
    Esen = Esen + Mass(i)*cL*(y(i)-Tm);
    dSdt(i) = Mass(i)*cL*dy(i)/y(i);
end
for i = LST-Ns+1:LST
    Mass(i) = 2*A(i)*2*dsld*rhoS;
    TPCMavg = TPCMavg + Mass(i)*y(i);
    MassPCM = MassPCM + Mass(i);
    Esen = Esen + Mass(i)*cL*(y(i)-Tm);
    dSdt(i) = Mass(i)*cL*dy(i)/y(i);
end
TPCMavg = TPCMavg/MassPCM;
Mass(1) = 2*A(1)*twh*7900;
Mass(LST+1) = 2*A(LST+1)*twh*7900;
Mass(LST+2) = 2*Aw*twh*7900;
Mass(LST+3) = 2*Aa*twh*7900;
Mass(LST+4) = 2*Ab*twh*7900;
dSdt(1) = Mass(1)*400*dy(1)/y(1);
dSdt(LST+1) = Mass(LST+1)*400*dy(LST+1)/y(LST+1);
```

```
dSdt(LST+2) = Mass(LST+2)*400*dy(LST+2)/y(LST+2);
dSdt(LST+3) = Mass(LST+3)*400*dy(LST+3)/y(LST+3);
dSdt(LST+4) = Mass(LST+4)*400*dy(LST+4)/y(LST+4);
dSdt(Nelm) = dV*rhoL*hsl/Tm;
Esen = Esen + Mass(1)*400*(y(1)-Tm);
Esen = Esen + Mass(LST+1)*400*(y(LST+1)-Tm);
Esen = Esen + Mass(LST+2)*400*(y(LST+2)-Tm);
Esen = Esen + Mass(LST+3)*400*(y(LST+3)-Tm);
Esen = Esen + Mass(LST+4)*400*(y(LST+4)-Tm);

Sdotin = qin1/(Tsath);
Sdotout = loadw1/(Tsw) + loadH1/(Tsa) + loadC1/(Tsb);
Qdotout = loadw1 + loadH1 + loadC1;
Qdotin = qin1;
Exin = qin1*(1-300/Tsath);
Exout = loadw1*(1-300/Tsw) + loadH1*(1-300/Tsa) + loadC1*(1-300/Tsb);
Load_Solar = [NHP*(loadw1+loadH1+loadC1) NHP*qin];
dms=max(0,totalload-totalqsolar);

%%%*************************** Superheat subroutine ****************

function [dy]= supheat(t,y)

global ri ro r twh kw Nelm Ns Nl LST NHP
global tallmelt STATE Sdotin Sdotout Qdotout Qdotin Exin Exout dSdt
global Lh Lw La Lb aw
global Tm hsl kL kS cL aL aS rhoL rhoS Esen Load_Solar
global Ti dlqd dsld A Mass TPCMavg
global totalqsolar totalload Qaux dms

hw = 2000;
ha = 500;
hb = 0.0;

mdotw = 0.0;
mdota = 0.0;
cpw = 4200;
cpa = 1000;
Tinw = 20;
Tina = 20;
TLiBr = 80;

%***********************************

loadC=[];
loadH=[];
loadw=[];
qsolar=[];
Asolar=;

tday = floor(t/3600)+1;
% if mod(tday,24)==1 %%% to start a new day
%     tday=1;
% end
if mod(tday,8760)==1
     tday=8760;
```

```
end
tday0 = tday-1;
if tday0==0
    tday0 = 8760;
end

tfrac = (t/3600)-floor(t/3600);
qsolart = qsolar(tday0)+tfrac*(qsolar(tday)-qsolar(tday0));
loadwt = (loadw(tday0)+tfrac*(loadw(tday)-loadw(tday0)))*1000;
loadHt = (loadH(tday0)+tfrac*(loadH(tday)-loadH(tday0)))*1000;
loadCt = (loadC(tday0)+tfrac*(loadC(tday)-loadC(tday0)))*1000;
%Tsath = max(300,y(1) + qin1*(twh/2)/(kw*pi*(2*ri-twh)*Lh));
qin = qsolart*Asolar*0.6;          % collector area = 10 m2; efficiency 60%
qin1 = qin/NHP;

Tsath = (y(1) + qin1*(twh/2)/(kw*pi*(2*ri-twh)*Lh));
if Tsath>=383.15
    qin=0;
    qin1 = qin/NHP;
    Tsath=y(1);
end
Qaux=0;
%*****************************************************************
dy = zeros(Nelm,1);
Aw = A(LST+1)*Lw/Lh;
Aa = A(LST+1)*La/Lh;
Ab = A(LST+1)*Lb/Lh;

Ti(1) = Tsath;
Ti(2) = (y(1)*kw*A(1)/(twh/2)+y(2)*kL*A(2)/dlqd)/...
    (kw*A(1)/(twh/2)+kL*A(2)/dlqd);
dlqd1 = A(Nl+1) - ri;
Ti(Nl+2) = (y(Nl+1)*kL*A(Nl+1)/dlqd1+y(LST+1)*kw*A(LST+1)/(twh/2))/...
    (kw*A(LST+1)/(twh/2)+kL*A(Nl+1)/dlqd1);

for i = 2:Nl+1
    if i == Nl+1
        Ti(i+1) = (y(Nl+1)*kL*A(Nl+1)/dlqd1+y(LST+1)*kw*A(LST+1)/(twh/2))/...
            (kw*A(LST+1)/(twh/2)+kL*A(Nl+1)/dlqd1);
    else
        Ti(i+1) = (y(i)*A(i)+y(i+1)*A(i+1)) / (A(i)+A(i+1));
    end
    dy(i) = (Ti(i) - 2*y(i) + Ti(i+1)) * aL/(2*dlqd^2);
end
dy(Nl+2:LST) = 0;
Tsatc=(y(LST+1)*A(LST+1)+y(LST+2)*Aw+y(LST+3)*Aa+y(LST+4)*Ab)/(A(LST+1)+Aw+Aa+A
b);

loadw1 = loadwt/NHP;
loadH1 = loadHt/NHP;
loadC1 = loadCt/NHP;
totalqsolar = qsolart*Asolar*0.6;
totalload = loadwt+loadHt+loadCt;

if Tsatc<=300
    Qaux=totalload;
    loadw1=0;
```

```
    loadH1=0;
    loadC1=0;
 end

%*************************************************
dy(1) = (Tsath - 2*y(1) + Ti(2)) * aw/(2*(twh/2)^2);
dy(Nl+1) = (Ti(Nl+1) - y(Nl+1))/dlqd - (y(Nl+1) - Ti(Nl+2))/dlqd1;
dy(Nl+1) = aL*dy(Nl+1)/(dlqd1+dlqd);
dy(LST+1) = (Ti(Nl+2) - 2*y(LST+1) + Tsatc) * aw/(2*(twh/2)^2);

%*******************************
Tsw = y(LST+2)-loadw1*(twh/2)/(kw*Aw*2*pi*Lh);
Tsb = y(LST+4)-loadH1*(twh/2)/(kw*Ab*2*pi*Lh);
Tsa = y(LST+3)-loadC1*(twh/2)/(kw*Aa*2*pi*Lh);
%*******************************
Tsw = real(Tsw);
Tsw = min(y(LST+2),Tsw);
Tsa = min(y(LST+3),Tsa);
%Tsb = (y(LST+4)*kw/(twh/2) + TLiBr*hb)/(kw/(twh/2) + hb);
Tsb = min(y(LST+4),Tsb);

dy(LST+2) = (Tsw - 2*y(LST+2) + Tsatc) * aw/(2*(twh/2)^2);
dy(LST+3) = (Tsa - 2*y(LST+3) + Tsatc) * aw/(2*(twh/2)^2);
dy(LST+4) = (Tsb - 2*y(LST+4) + Tsatc) * aw/(2*(twh/2)^2);

if (t>5 && mod(t,300)<1.0)
    if (y(end)<=ro-ri)
        M = (y(end)+ri)^2-ri^2;
    else
        M = ro^2-ri^2 + ro^2 - (2*ro-(y(end)+ri))^2;
    end
    f = M/(2*(ro^2-ri^2));
    yo=1;
    [t/3600 y(1) y(LST+1) y(end)*1000 f qin/1000-(loadHt+loadwt+loadCt)/1000 Nl
Ns TPCMavg]
end

dSdt = zeros(Nelm,1);
TPCMavg = 0;
MassPCM = 0;
Esen = 0;
for i = 2:Nl+1
    Mass(i) = 2*A(i)*2*dlqd*rhoL;
    if i==Nl+1
        Mass(i) = ((A(i)+dlqd)^2-ri^2)*rhoL;
    end
    TPCMavg = TPCMavg + Mass(i)*y(i);
    MassPCM = MassPCM + Mass(i);
    Esen = Esen + Mass(i)*cL*(y(i)-Tm);
    dSdt(i) = Mass(i)*cL*dy(i)/y(i);
end
TPCMavg = TPCMavg/MassPCM;
Mass(1) = 2*A(1)*twh*7900;
Mass(LST+1) = 2*A(LST+1)*twh*7900;
Mass(LST+2) = 2*Aw*twh*7900;
Mass(LST+3) = 2*Aa*twh*7900;
Mass(LST+4) = 2*Ab*twh*7900;
```

```
dSdt(1) = Mass(1)*400*dy(1)/y(1);
dSdt(LST+1) = Mass(LST+1)*400*dy(LST+1)/y(LST+1);
dSdt(LST+2) = Mass(LST+2)*400*dy(LST+2)/y(LST+2);
dSdt(LST+3) = Mass(LST+3)*400*dy(LST+3)/y(LST+3);
dSdt(LST+4) = Mass(LST+4)*400*dy(LST+4)/y(LST+4);
Esen = Esen + Mass(1)*400*(y(1)-Tm);
Esen = Esen + Mass(LST+1)*400*(y(LST+1)-Tm);
Esen = Esen + Mass(LST+2)*400*(y(LST+2)-Tm);
Esen = Esen + Mass(LST+3)*400*(y(LST+3)-Tm);
Esen = Esen + Mass(LST+4)*400*(y(LST+4)-Tm);

Sdotin = qin1/(Tsath);
Sdotout = loadw1/(Tsw) + loadH1/(Tsa) + loadC1/(Tsb);
Qdotout = loadw1 + loadH1 + loadC1;
Qdotin = qin1;
Exin = qin1*(1-300/Tsath);
Exout = loadw1*(1-300/Tsw) + loadH1*(1-300/Tsa) + loadC1*(1-300/Tsb);
Load_Solar = [NHP*(loadw1+loadH1+loadC1) NHP*qin1];
dms=max(0,totalload-totalqsolar);
```